Office de la Propriété Intellectuelle du Canada
Un organisme d'Industrie Canada

Canadian Intellectual Property Office
An agency of Industry Canada

CA 2851633 A1 2015/11/12

(21) 2 851 633

(12) DEMANDE DE BREVET CANADIEN
CANADIAN PATENT APPLICATION

(13) A1

(22) **Date de dépôt/Filing Date:** 2014/05/12

(41) **Mise à la disp. pub./Open to Public Insp.:** 2015/11/12

(51) **Cl.Int./Int.Cl.** ***B28B 19/00*** (2006.01),
C01G 23/04 (2006.01), ***C01G 37/02*** (2006.01),
C04B 35/46 (2006.01), *C23C 24/08* (2006.01)

(71) **Demandeur/Applicant:**
NATIONAL RESEARCH COUNCIL OF CANADA, CA

(72) **Inventeur/Inventor:**
UNKNOWN, ZZ

(74) **Agent:** LEMAY, CATHERINE

(54) **Titre : REVETEMENTS NANOSTRUCTURES DE TI02-CR2O3 PULVERISES PAR TRAITEMENT THERMIQUE**
(54) **Title: NANOSTRUCTURED TIO2-CR2O3 THERMAL SPRAYED COATINGS**

(57) **Abrégé/Abstract:**
Thermal sprayed ceramic coatings are successfully employed to enhance the load carrying capacity and the tribological performance of the base material in order to extend the in-service life of equipment, including metal-seated ball valves (MSBV's) in Hydrometallurgy service. Ceramic coatings are vital to protect machines in the harsh abrasive conditions encountered in corrosive processes such as Pressure Oxidation (POx) and High Pressure Acid Leach (HPAL). Velan, a leading designer and manufacturer of industrial valves, has 20 years of experience in the engineering of severe service MSBV's for critical isolation applications around the autoclave. The National Research Council of Canada (NRC) in Boucherville and Polytechnique Montreal have world recognized know-how on coating engineering and characterization, in particular for wear. A detailed characterization project was undertaken by Velan in collaboration with the NRC and Polytechnique Montreal to perform mechanical and tribological resistance evaluation of the most promising ceramic coatings potentially suitable for this service, including a novel blend of n-TiO_2-Cr_2O_3. Hardness and shear strength were evaluated using micro-hardness indentation testers and universal tensile testing equipment. Wear resistance of the coatings under different conditions such as sliding wear, abrasion and galling were measured by standard pin-on-disc tests, abrasion tests and custom-design galling tests. It was found that TiO_2-Cr_2O_3 offers superior tribological performances compared to n-TiO_2, mainly due to the presence of Cr_2O_3. Optimized balance between the hard and brittle Cr_2O_3 phases and the soft and ductile TiO_2 phases yields to higher abrasion, sliding and galling resistance. In parallel, the novel mix of n-TiO_2, and Cr_2O_3 is considered as a promising evolution of the current TiO_2-Cr_2O_3 blend.

NANOSTRUCTURED AND CONVENTIONAL Cr_2O_3, TiO_2 AND TiO_2-Cr_2O_3 THERMAL SPRAYED COATINGS FOR METAL SEATED BALL VALVE APPLICATIONS IN HYDROMETALLURGY

By

[1]Luc Vernhes, Craig Bekins, Nicolas Lourdel,

[1]Velan, Canada

[2]Dominique Poirier, Rogerio S. Lima

[2]National Research Council of Canada, Canada

[3]Duanjie Li, Jolanta E. Klemberg-Sapieha

[3]Polytechnique Montreal, Canada

Presenter and Corresponding Author

Luc Vernhes
luc.vernhes@velan.com

ABSTRACT

Thermal sprayed ceramic coatings are successfully employed to enhance the load carrying capacity and the tribological performance of the base material in order to extend the in-service life of equipment, including metal-seated ball valves (MSBV's) in Hydrometallurgy service. Ceramic coatings are vital to protect machines in the harsh abrasive conditions encountered in corrosive processes such as Pressure Oxidation (POx) and High Pressure Acid Leach (HPAL).

Velan, a leading designer and manufacturer of industrial valves, has 20 years of experience in the engineering of severe service MSBV's for critical isolation applications around the autoclave. The National Research Council of Canada (NRC) in Boucherville and Polytechnique Montreal have world recognized know-how on coating engineering and characterization, in particular for wear.

A detailed characterization project was undertaken by Velan in collaboration with the NRC and Polytechnique Montreal to perform mechanical and tribological resistance evaluation of the most promising ceramic coatings potentially suitable for this service, including a novel blend of n-TiO_2-Cr_2O_3. Hardness and shear strength were evaluated using micro-hardness indentation testers and universal tensile testing equipment. Wear resistance of the coatings under different conditions such as sliding wear, abrasion and galling were measured by standard pin-on-disc tests, abrasion tests and custom-design galling tests.

It was found that TiO_2-Cr_2O_3 offers superior tribological performances compared to n-TiO_2, mainly due to the presence of Cr_2O_3. Optimized balance between the hard and brittle Cr_2O_3 phases and the soft and ductile TiO_2 phases yields to higher abrasion, sliding and galling resistance. In parallel, the novel mix of n-TiO_2 and Cr_2O_3 is considered as a promising evolution of the current TiO_2-Cr_2O_3 blend.

Thermal sprayed ceramic coatings are successfully employed to enhance the load carrying capacity and the tribological performance of the base material in order to extend the in-service life of equipment, including metal-seated ball valves (MSBV's) in Hydrometallurgy service. Ceramic coatings are vital to protect machines in the harsh abrasive conditions encountered in corrosive processes such as Pressure Oxidation (POx) and High Pressure Acid Leach (HPAL).

Pressure Oxidation (POx) and High Pressure Acid Leach (HPAL) are mineral recovery processes where the ore is leached using sulphuric acid into an autoclave at high pressure (up to 4.1 bar) and elevated temperatures (up to 240°C). The valves required to operate in this corrosive environment are manufactured with either titanium or duplex stainless steel substrates with their sealing surfaces protected with a ceramic coating, typically deposited via thermal spray processing. The primary function of the ceramic coating is to enhance the load carrying capacity and the tribological performance of the base material in order to extend the in-service life of the equipment, especially during ball motion phases.

Over the years, the industry has been working to optimize ceramic coating solutions, typically via thermal spray processing, for this type of application. One engineering firm has utilized a nanostructured TiO_2 coating, which has worked reasonably well at Ravensthorpe - Australia and Ramu - Papua New Guinea.

The two today ceramic coatings have limitations:
1) Pure TiO2 (conventional and nanostructured) ceramics have limited mechanical and tribological performances, leading to high wear rates.
2) TiO2-Cr2O3 offers superior tribological performances compared to TiO2, mainly due to the presence of Cr2O3. Optimized balance between the hard and brittle Cr2O3 phases and the soft and ductile TiO2 phases yields to higher abrasion, sliding and galling resistance. However, maintenance required on Pox and HPAL valves represent a significant percentage of the total operating budget. Technical innovation is needed to reduce maintenance in order to lower total cost of valve ownership.

It is proposed to use a blend of a conventional Cr_2O_3 powder and a nanostructured TiO2 powder (n-TiO2-Cr2O3) as a feedstock to plasma spray. An example of a ratio investigated is 55 wt% nTiO2/45 wt% Cr_2O_3. However, it is believed that this ratio could be adjusted for specific needs. Coatings produced out of this blend can provide superior mechanical and tribological performance than current ceramics used. Table 1 below summarizes the mechanical and wear performance data of several ceramic coatings. "NRC-5" is a typical n-TiO2 coating produced by plasma spray. "DS-2" is the TiO2-Cr_2O_3 coating currently used by Velan for its ball-valve. "NRC-1" is the coating proposed as an invention. It can be seen that this last coating offers hardness and wear resistance levels far higher than those currently achieved by the "state-of-the-art" coatings. The performances of n-TiO2-Cr_2O_3 are explained by the combination of the hard Cr_2O_3 phase with the n-TiO2, which is providing enhanced toughness. The nano-zones present in n-TiO2 and made of non-molten nanostructured particles have been found to act as crack arresters in previous studies (R.S. Lima). N-TiO2-Cr203 coating has also been produced using Mettech Axial III air plasma spray (APS) thermal spray system, which is a high power torch that can provide high in-flight particle speed, known to contribute to overall coating quality.

Table 1: Mechanical and Wear Performance Data

Coating	Torch (composition)	Microhardness (HV-300gf, n=10)	Abrasion Volume loss with method B-mod (mm³, n=2)	Wet Abrasion Resistance	Sliding Wear Rate ($mm^3/N.m$)	Galling Resistance
NRC-1	Mettech ($n\text{-}TiO_2\text{-}Cr_2O_3$)	1200 ± 49	7.8 ± 0.6	+++	10^{-6}	+++
NRC-5	Mettech ($n\text{-}TiO_2$)	729 ± 45	31.6 ± 0.6	++	10^{-4}	++
DS-2	SG100 ($TiO_2\text{-}Cr_2O_3$)	912 ± 42	20.5 ± 0.5	+	3×10^{-5}	+

In order to fully benefit of the blend composition n-TiO2-Cr2O3, the spraying parameters must be carefully adjusted to optimize coating behaviour. n-TiO2 and Cr2O3 particles/materials exhibit different thermal and mechanical properties (e.g., melting point, thermal conductivity, hardness, elastic modulus and toughness), which influence thermal spray deposition characteristics and wear performance levels, as well as, corrosion resistance. There should be a window of processing where the n-TiO2 and Cr2O3 blend mixture, particle size distribution, particle temperature & velocity during spraying, dwell time of the particles in the spray jet yield an optimized coating microstructure for this application. As a consequence, this invention includes the specific spraying parameters required to reach the optimised coating properties.

INTRODUCTION

Over the last two decades, metal-seated ball valves (MSBV's) have become the industry standard for Hydrometallurgy application, providing tight, reliable shut-off in this critical service which facilitates maintenance and contributes to a safe working environment. Typical MSBV's design for this application consists of a floating ball in contact with a fixed seat. Ball and seats are manufactured with either titanium or duplex stainless steels substrates and protected with a ceramic coating. The primary function of the ceramic coating is to enhance the load carrying capacity and the tribological performance of the base material in order to extend the in-service life of the equipment, especially during ball motion phases.

Conventional Cr_2O_3 applied by Air Plasma Spray (APS) was the coating selected 20 years ago to protect MSBV's against the extreme abrasion, pressure and elevated temperature inherent to the Pressure Oxidation (POx) recovery process used for gold where the ore is mixed with oxygen and sulfuric acid into an autoclave. Over the years, based on field experiences, silicon dioxide and titanium dioxide have been gradually added to the originally pure Cr_2O_3 blend in order to improve its ductility and toughness. Velan's Cr_2O_3 blend has proved itself in gold extraction technologies such as Nerco's Con Gold mine - Canada, Barrick Goldstrike, and Lone Tree mines - USA. Lihir and Porgera Gold Mines in Papua - New Guinea's have also reported good experience with Velan Cr_2O_3 blend material applied to MSBV's[(1)].

Similar to POx, High Pressure Acid Leach (HPAL) is a recovery process for nickel where the laterite ore is leached in a sulfuric acid environment into an autoclave at 4.1 bar (600 psi) and temperatures above 240°C (464°F). Unlike POx, HPAL process operates at high pressure that, combined with a higher chloride content, leads to a more corrosive environment (i.e. Titanium is susceptible to crevice corrosion in HPAL). Based on Velan's experience with different coating blends at Falconbridge mines - Canada, Cr_2O_3 blend optimized for POx corrodes prematurely when used in HPAL. Being relatively inert in such an environment, TiO_2 seems an instinctive choice for HPAL[(2)]. However, conventional TiO_2 mechanical and tribological performances are significantly lower than those of Cr_2O_3 leading to higher wear rates, as experienced by Velan at Cawse and Murin-Murin nickel mines - Australia.

The industry has been working to optimize coating solutions for HPAL[(3)]. Several options have been considered and unsuccessfully tested by different companies to mitigate corrosion. This includes the use of intermediate bond coats, such as gold and tantalum, in between the base material and the Cr_2O_3 top coat. One engineering firm has utilized a nanostructured TiO_2 coating, which has worked reasonably well at Ravensthorpe – Australia and Ramu – Papua New Guinea[(4,5)]. At the same time, Velan has developed a proprietary ceramic blend containing TiO_2 and Cr_2O_3 in order to get the corrosion resistance of a pure TiO_2 and the tribological performances of Cr_2O_3. This coating has demonstrated superior performance on several HPAL projects, including Coral Bay - Philippines, Goro - New Caledonia and Ambatovy – Madagascar[(1)]. All critical isolation valves installed on the recent Taganito - Philippines project have also been supplied with this optimized TiO_2-Cr_2O_3 blend.

In collaboration with the NRC and Polytechnique Montreal, a detailed characterization project was undertaken by Velan to perform mechanical and tribological resistance evaluations of the most promising ceramic coatings potentially suitable for Hydrometallurgy application, including a novel nano-structured blend of n-TiO_2-Cr_2O_3. All test results have been compiled to help Velan selecting the appropriate coating to optimize the MSBV's performance in POx and HPAL applications.

Section 2 describes experimental procedures, including materials and characterization techniques. Section 3 presents research findings and their analysis. Section 4 concludes.

EXPERIMENTAL

Material

Base Material

All coatings were applied onto titanium grade 5 coupons (ASTM B348) that were previously grit blasted (Al_2O_3 - grit 24). A nominal coating thickness of 0.020" (500 µm) was targeted.

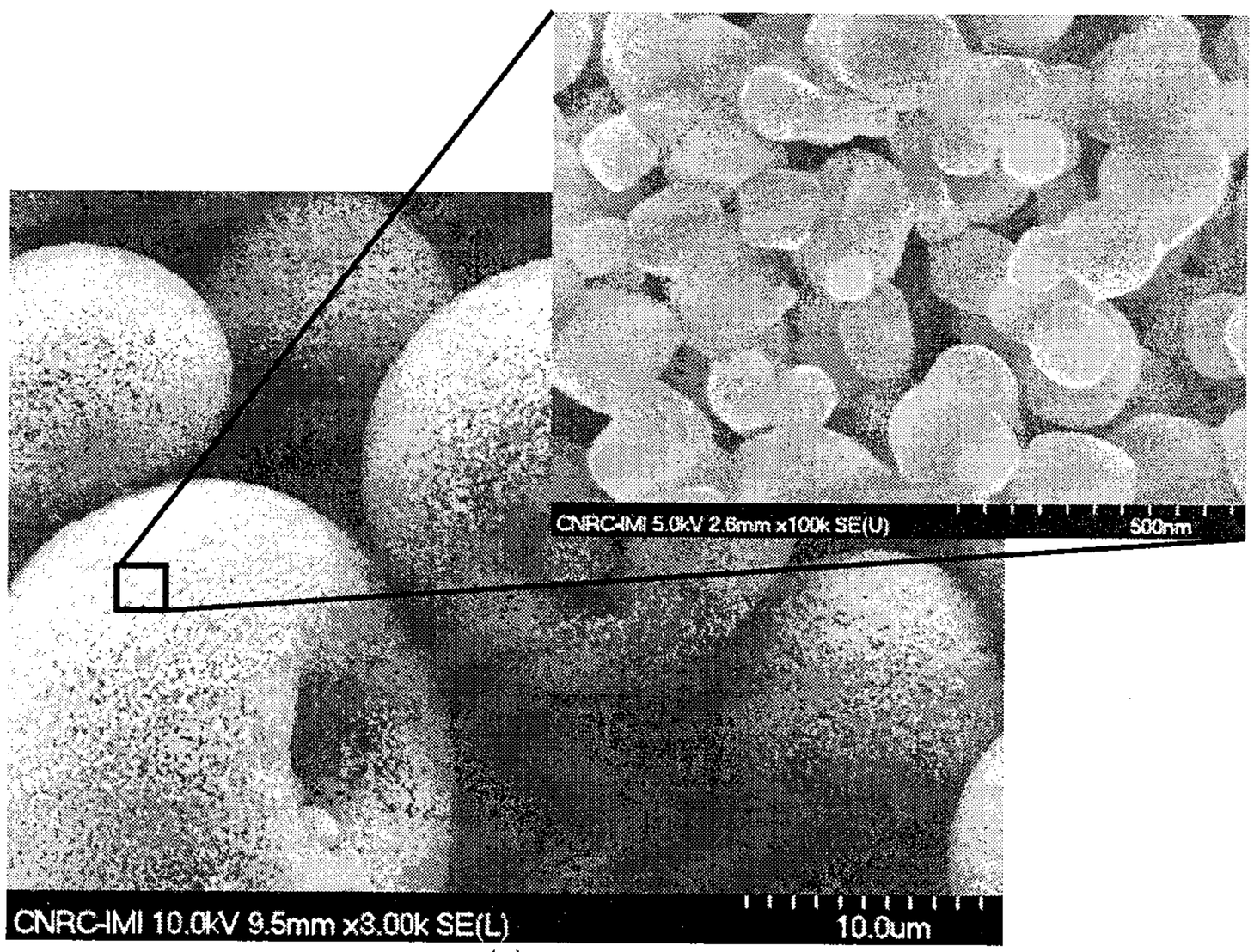
Powder Material

The following powder materials have been selected based on literature review and field experience:

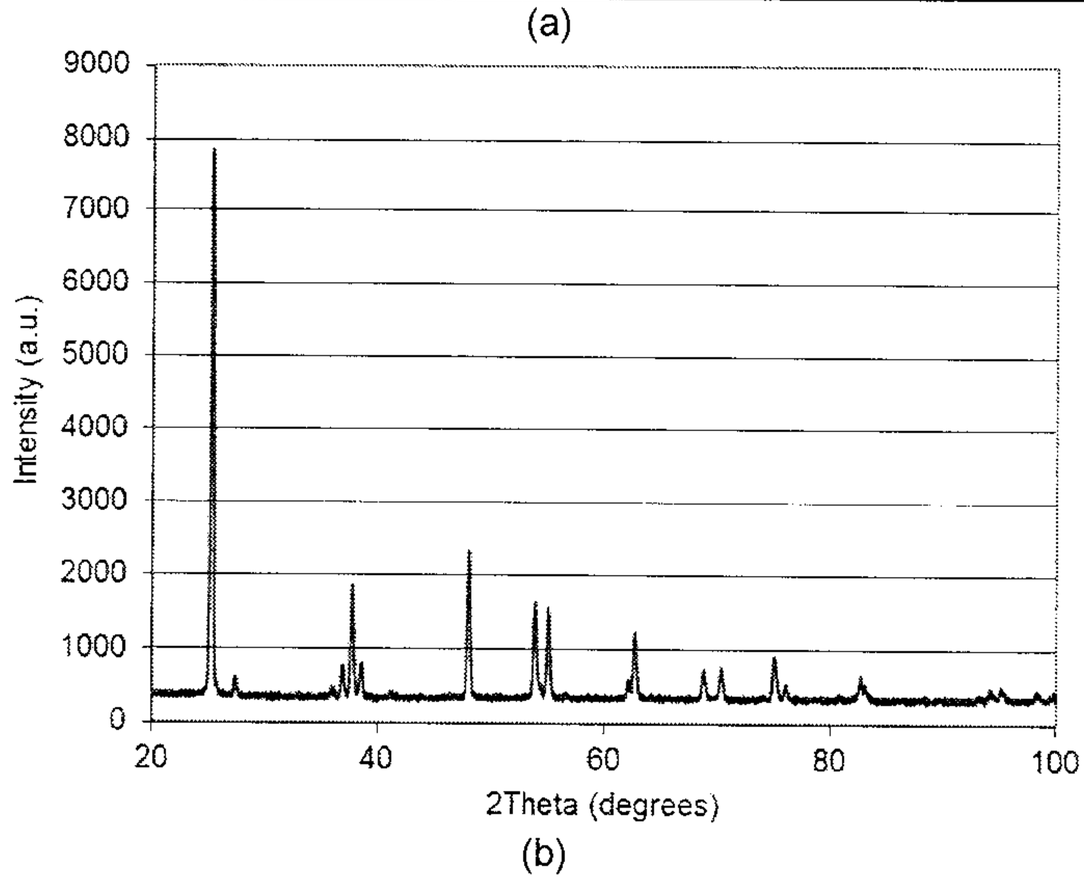
1) Cr_2O_3 (Velan proprietary blend),
2) TiO_2 - Cr_2O_3 (Velan proprietary blend),
3) n-TiO_2 (Millydine supplier),
4) n-TiO_2-Cr_2O_3 (Velan proprietary blend).

Cr_2O_3 and TiO_2 - Cr_2O_3 are current Velan proprietary ceramic coatings for Hydrometallurgy.

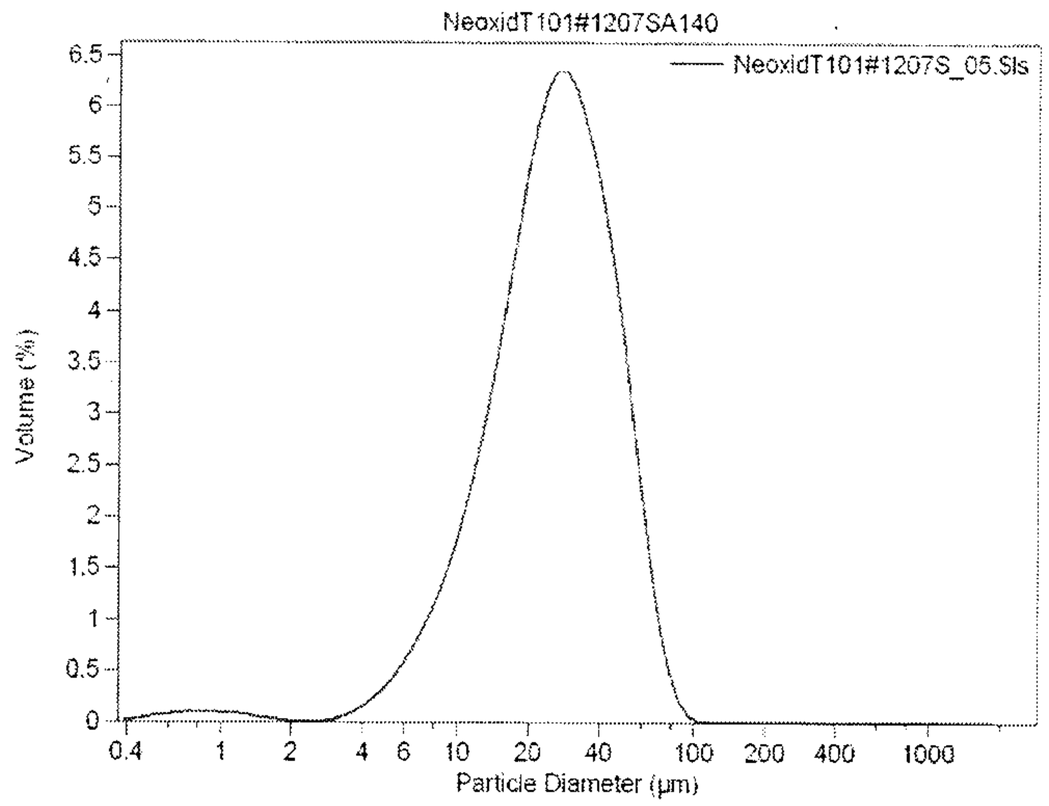
n-TiO2 is considered by the authors as the finest TiO_2 available on the market. This powder is formed from nanosize constituents agglomerated and sintered in bigger particles to allow spraying. *Figure 1* is showing n-TiO_2 powder microstructure, together with the XRD and size distribution of those particles (laser diffraction particle size analyzer).



(a)



(b)



(c)

Figure 1: n-TiO_2 powder characteristics (a) SEM micrographs (b) XRD pattern and (c) particle size distribution - logarithmic scale

Finally a novel blend of n-TiO_2 and Cr_2O_3 has been developed by the authors especially for this project. n-TiO_2 powder from Millydine was mixed with Metco 106, which is a fused, sintered and crushed Cr_2O_3 powder.

Deposition Techniques

High Velocity Oxygen Fuel (HVOF) and APS are the two dominant thermal spray processes used to apply these materials. APS, with an in-flight particle temperature around ~ 2,600°C (~ 4,700°F), is more appropriate to apply Cr_2O_3 (melting point around 2,350°C / 4,260°F) than HVOF (maximum in-flight particle temperature around 2,300°C / 4,172°F). Consequently, all coatings have been deposited with the APS process.

Velan proprietary blends were deposited using the SG100 torch from Praxair as presented in Table 1. n-TiO_2 and n-TiO_2-Cr_2O_3 coatings were deposited using high power Mettech Axial III APS torch. Regarding n-TiO_2 feedstock, a previous NRC study had identified the best set of spraying parameters for sliding wear performance. The same set was selected for this study. For n-TiO_2-Cr_2O_3 powder blend, the gas flows, current and spraying distances were varied in order to produce coatings with different structures and properties (preliminary trials). The parameter set that produced the hardest and toughest coating was selected for coating production.

The different spraying parameters are presented in *Table 1*. In-flight particle temperature and velocity were measured by the thermal spray sensor DPV 2000 (Tecnar Automation).

Table 1: Spraying Parameters

	Cr_2O_3	TiO_2 - Cr_2O_3	n-TiO_2	n-TiO_2 - Cr_2O_3
Torch	SG-100	SG-100	Mettech Axial III	Mettech Axial III
Ar flow (lpm)	53	53	37.5	62.5
H_2 flow (lpm)	*Confidential*		37.5	62.5
N_2/He flow (lpm)	41 He	41 He	75 N_2	125 N_2
Current (A)	800	800	230*	230*
Voltage (V)	~ 42	~ 42	152	205
Power (kW)	33.6	33.6	105	141
Net Power (kW) or Enthalpy (kJ/L)	*Confidential*		15.0 kJ/L	18.2 kJ/L
Nozzle	730 Anode / 129 Cathode	730 Anode / 129 Cathode	3/8"	3/8"
Spraying Distance (cm)	6.35	6.35	14	14
Feedrate (g/min)	~30	~30	18	18
Ar Carrier Gas (lpm)	5	5	9	9
In-flight Temperature (°C)	*Confidential*		2578±166**	2590±258**
In-flight Velocity (m/s)			269±45**	457***±91**

*Current per electrode set – 3 electrode sets in the torch.
**The standard deviation corresponds to the sample distribution, and not the experimental error.
***Approximation; velocity higher than the standardized range.

Characterization Techniques

Microstructure

Microstructures of the coatings were obtained with a JSM-6100 SEM from JEOL or the FE-SEM Hitachi S4700, under back-scattered electron (BSE) mode. EDS analyses were performed using JEOL JSM-840 SEM. Coatings were sectioned with a coolant-assisted diamond wheel and then cold vacuum mounted in an epoxy resin. Grinding and polishing were done using standard metallographic preparation procedures

Mechanical Property Characterization

Micro-Hardness and shear strength were evaluated using respectively micro-hardness indentation testers and universal tensile testing equipment.

Microhardness measurements were performed on coating polished cross-sections with a Buehler Micromet II Tester (Vickers Tip) under a 300 gf load. For each specimen, a minimum of 12 indentations was performed (straight line pattern, at the center of the coating cross section), and the highest and lowest values removed from the dataset.

Coating adhesion on Ti substrate was assessed through shear tests (ASTM F1044 respectively). An Instron 5582 universal testing machine was used to determine the maximum shear loads required to obtain sample separation.

Tribological Behavior Evaluation

Wear resistance of the coatings under different conditions such as sliding wear and abrasion were measured by standard pin-on-disc tests and abrasion tests. Galling resistance was measured using a custom-designed and automated galling tester.

Sliding Wear Resistance

A custom-made pin-on-disc tribometer was employed to evaluate the sliding wear behavior of the coatings. A normal load of 25 N was applied to a tungsten carbide ball (4.75 mm diameter) used as a counterpart material. A new ball was used for each test. The diameter of the wear track ring, d,

was 7 mm and the rotation speed was 546 revolutions per minute (rpm). This results in a linear speed of 20 cm/s. (7.9 in/s.). The coefficient of friction, COF, was recorded every second during the test. The wear rate, K, was evaluated using the formula K=V/(F×s), where V is the worn volume, F is the normal load, and s is the sliding distance. Pin-on-disc wear track profiles were evaluated by the Sloan Dektak II profilometer, and the wear track morphology was examined by optical microscopy (Nikon Epiphot 200).

Dry Sand Abrasion Resistance

Coating dry abrasion resistance was tested through dry sand/rubber wheel abrasion test (ASTM G65 / procedure D-modified, 45 N, 2000 wheel revolutions, Durometer A-60 wheel). Two samples were tested for each coating type. Prior testing, the sample surfaces were ground with diamond wheel to produce a surface finish of about 0.2-0.3 µm. Evaluation of the sample volume loss due to the test was performed with an optical profilometer.

Wet Sand Abrasion Resistance

Coating wet abrasion resistance by means of wet sand / rubber wheel was measured following ASTM G105-02 modified procedure guidelines using a Falex® sand abrasion test machine and controlled slurry. For each coating type, one rectangular shape specimen (1" x 3" x 0.5") has been submitted to a 5,000 cycles run with 22 N normal load using a 7" diameter and Durometer A-60 neoprene rubber wheel at a nominal speed of 245 rpm. The slurry mixture was composed of rounded quartz grain sand AFS 50/70 and deionized water with respect to the ratio of 0.940 kg water / 1.500 kg sand. Prior testing, the sample surfaces were ground with diamond wheel to produce a surface finish of about 0.2-0.3 µm. Test allowed for ranking coating that resists penetration to its substrate while wet abrasion rate has been reported as mass loss (accuracy +/- 0.1 mg) of the specimen.

Variable Temperature Galling Resistance

Galling resistance was measured using a custom-designed and automated galling tester developed by Engineered Valve International Inc. in collaboration with Velan (see *Figure 2*). The tester consists in quarter-turn rotating an annular coated specimen (dia. 1.25" x 1.5" thickness, 1 in^2 coated surface) against a second annular coated and fixed specimen under controlled contact pressure, stroke motion and temperature conditions. Contact load and stroke motions are respectively applied with a pneumatic thrust actuator (Samson 3277) and a quarter-turn actuator (Metso B1CU6/20L) while the temperature is adjusted with a radiation-type furnace (Lindberg Blue M Tube Furnace) coupled with a K-Type thermocouple probe tack-welded on one specimen. All test parameters are controlled from a centralized panel. Coated surface of each specimen is successively prepared and inspected before being tested. The coated surface preparation consists in manually polishing with several grades of polishing clothes (from P320 to P1200 grit) using a thin buffer of commercial machinery oil. The specimen inspection allows for selecting specimens presenting a surface roughness R_a below 10 µin with a flatness below 0.005 inch in addition to measuring the specimen mass (+/- 0.5 mg). For each coating type, one set of two self-mated specimens has been tested according to the procedure detailed in *Table 2*. The test procedure is stopped as soon as one coated specimen displays significant wear pattern (ex.: micro-welding, scoring). Repeating this test procedure for each coating type allows material ranking based on galling resistance and total mass loss over a given period.

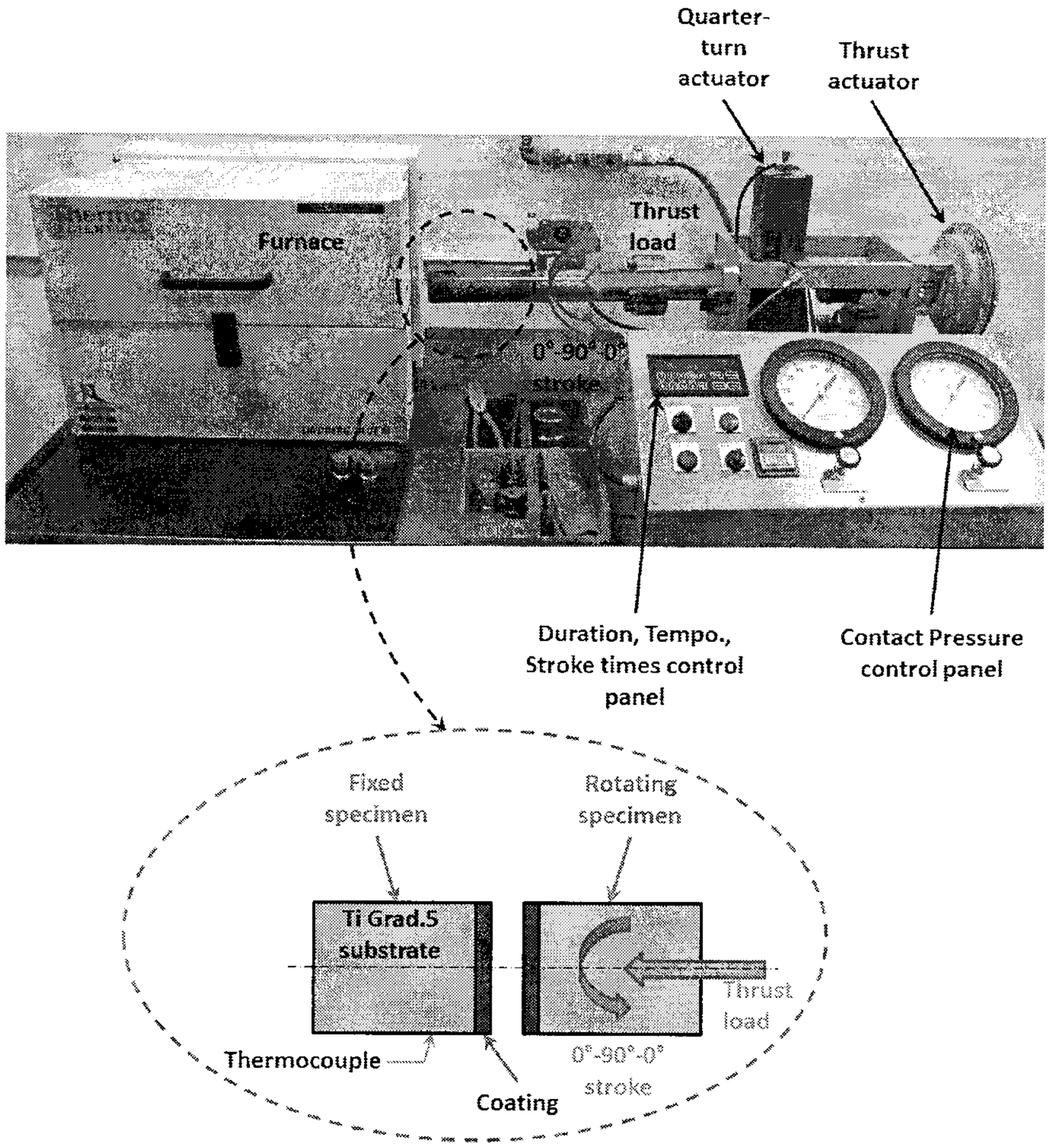


Figure 2: Custom-designed and automated variable temperature galling tester

Table 2: Variable temperature galling test procedure

Step	Duration (nb. cycles)	Specimen temperature, °C (*°F*)	Nominal contact pressure, MPa (*psi*)	Nb. cycles per minute	0° ⊠ 90° and 90° ⊠ 0° stroke times (s.)	Temporization at 0° and 90° position (s.)
1	50	R.T.	6.9 MPa +/- 0.3 (*1,000 +/- 50*)	0.2	10 +/- 0.5	140
2	50	220 +/- 7 * (*428 +/- 12*)	6.9 MPa +/- 0.3 (*1,000 +/- 50*)	0.2	10 +/- 0.5	140
3	50	220 +/- 7 * (*428 +/- 12*)	10.3 MPa +/- 0.3 (*1,500 +/- 50*)	0.2	10 +/- 0.5	140
4	50	220 +/- 7 * (*428 +/- 12*)	13.8 MPa +/- 0.3 (*2,000 +/- 50*)	0.2	10 +/- 0.5	140

*: Heating ramps are adjusted to 204°C (400°F) per hour.

RESULTS AND DISCUSSIONS

Microstructure

The microstructure of Cr_2O_3, TiO_2, n-TiO_2 and n-TiO_2-Cr_2O_3 coatings are shown in *Figure 3*. The two phases present in the coatings with the blend powder feedstock are Cr_2O_3 (light grey) and TiO_2 (dark grey) respectively. All coatings have shown low levels of porosity. Fine cracks seen in particles and at particle boundaries are thought to be formed due to quenching. The large cracks are typically formed as stress relief due to stresses from CTE mismatch with the substrate and/or residual stresses within the coating.

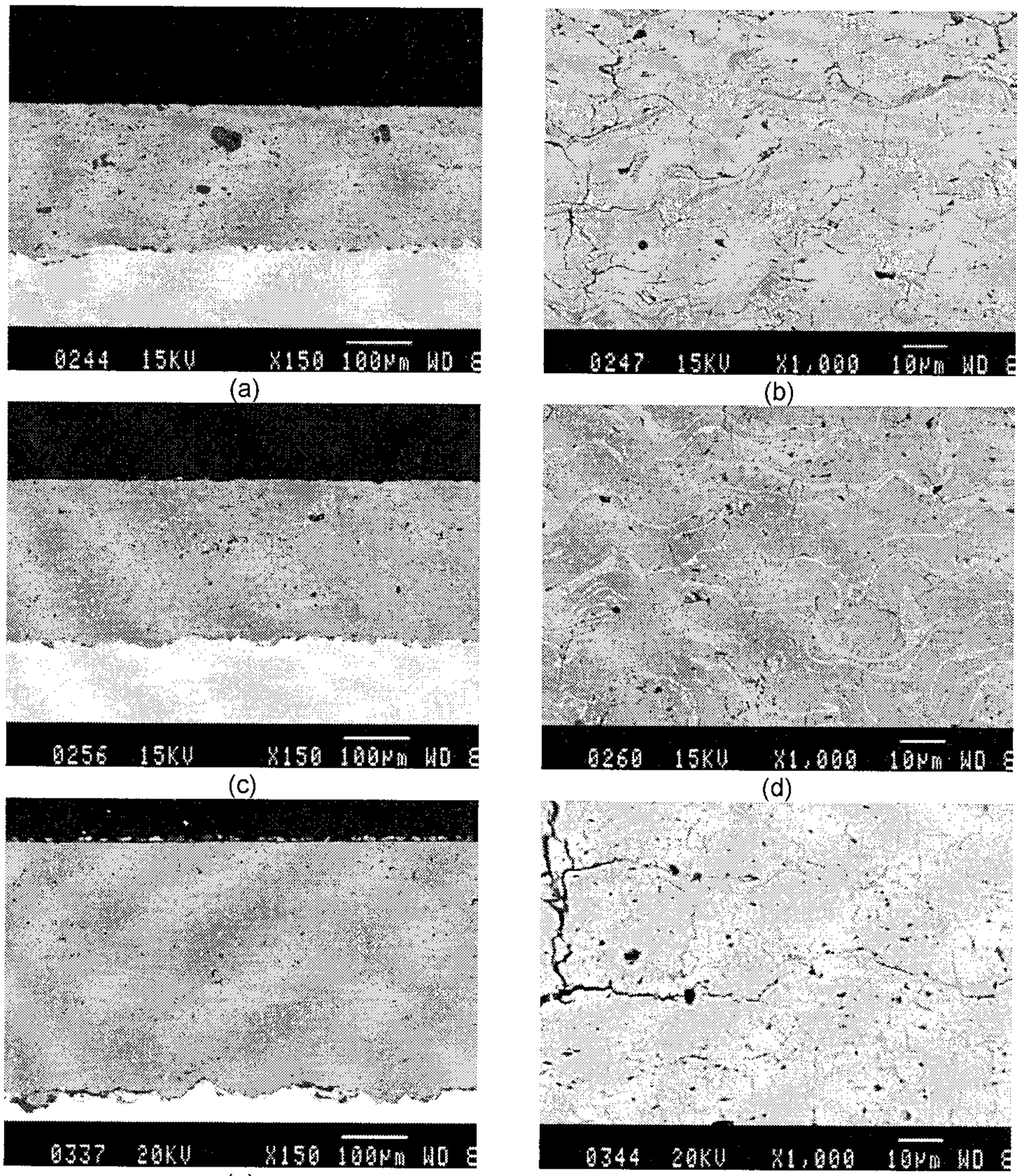


Figure 3: Coatings microstructure: Cr_2O_3 at (a) 150X and (b) 1000X. TiO_2-Cr_2O_3 at (c) 150X and (d) 1000X. n-TiO_2 at (e) 150X and (f) 1000X. n-TiO_2-Cr_2O_3 at (g) 150X and (h) 1000X

EDS spectra acquired from the four different coatings are shown in *Figure 4*. The chemical composition of each coating is confirmed.

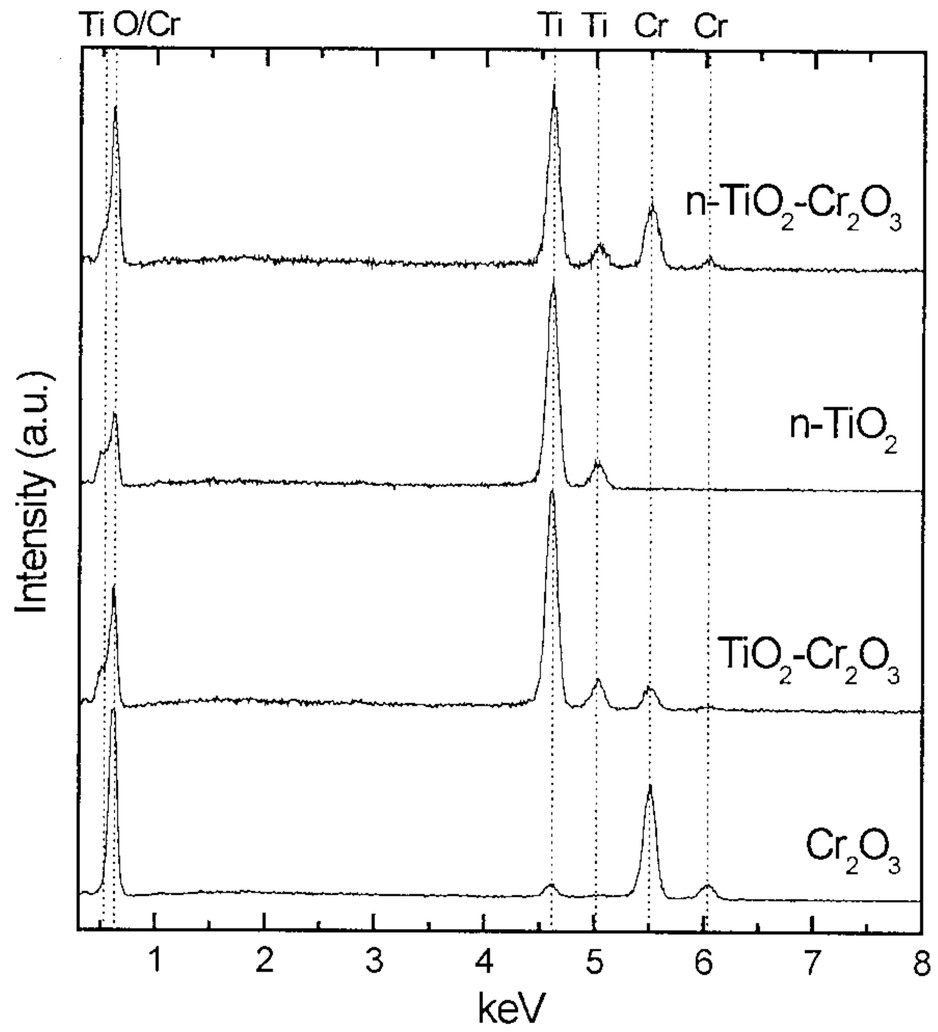


Figure 4. EDS spectra of Cr_2O_3, TiO_2 - Cr_2O_3, n-TiO_2 - Cr_2O_3 and n-TiO_2 - Cr_2O_3 materials

Microhardness

Microhardness values are shown in *Table 3.* As expected, the highest microhardness is achieved when the hardest phase, Cr_2O_3, is primary used for the coating. The second highest coating in microhardness is the n-TiO_2-Cr_2O_3.

Table 3: Coating properties

Coating	Microhardness (HV-300gf, n=10)	Dry Abrasion: Volume loss with method D-mod (mm^3, n=2)	Shear Strength (MPa, n=5)
Cr_2O_3	1423 ± 62	17.1 ± 2.1	> 42 ± 7 [d]
TiO_2-Cr_2O_3	912 ± 42	20.5 ± 0.5	> 46 ± 2 [b]
n-TiO_2	729 ± 45	31.6 ± 0.6	36 ± 2 [a]
n-TiO_2-Cr_2O_3	1200 ± 49	7.8 ± 0.6	38 ± 5 [a]

[a] Adhesive failure (occurs at bond line with substrate)
[b] Epoxy failure (glue)
[c] Cohesive failure (failure within the coating)
[d] Mix mode of all or partial of the above.
Please note it is not conceivable to have interface failure and epoxy failure and not have some cohesive failure.

The improved hardness of n-TiO_2-Cr_2O_3 compared to the conventional TiO_2-Cr_2O_3 is probably due to the use of the Mettech Axial III torch for spraying. The higher power of the torch together with the high gas flow used provides very high in-flight particle speed. High in-flight particle speed is known to contribute to overall coating quality[(6)].

Adhesion

All coatings produced were found to provide good bonding to the substrate. The best coating adhesion in shear is achieved with TiO_2-Cr_2O_3. Even though the variation in coating adhesion is relatively low, it can also be seen that n-TiO_2 and n-TiO_2-Cr_2O_3 coatings display lower adhesion.

This is believed to be due to the higher thickness of those coatings (*Table 1*). Thicker thermal sprayed coatings typically display lower adhesion due to the buildup of residual stresses[7].

Tribo-Mechanical Properties

Sliding Wear Resistance

The coefficient of friction, COF, as a function of the sliding distance is shown in *Figure 5*. It can be observed that in the first 500 m sliding distance, the COFs of different coatings exhibit a value in the range of 0.6 to 0.7. After the accommodation period (resulting in the high COF value of ~0.65 at the beginning of the wear test for Cr_2O_3), the COF of Cr_2O_3 progressively decreases and reaches a stable value of ~0.5. The COF of n-TiO_2-CrO_3 coating exhibits fluctuations ranging from ~0.6 to ~0.7 during its relatively long accommodation period, and it eventually reaches a value of ~0.6. In comparison, coatings TiO_2-Cr_2O_3 and n-TiO_2 show a trend of progressively increasing COFs from ~0.6 to ~0.7 and from ~0.7 to ~0.8, respectively.

Frictional behavior of various coatings correlates with their different wear resistance as shown in *Figure 6*. The Cr_2O_3 coating has a substantially enhanced wear resistance, showing a wear rate of ~5.5 x 10^{-8} $mm^3/(N.m)$. The n-TiO_2-Cr_2O_3 coating exhibits a low wear rate of ~1.3 x 10^{-6} $mm^3/(N.m)$. In contrast, coatings TiO_2-Cr_2O_3 and n-TiO_2 show wear rates of ~3.73 x 10^{-5} and ~7.6 x 10^{-5} $mm^3/(N.m)$, respectively, approximately three orders of magnitude higher compared to the Cr_2O_3 coating. This is in agreement with the microscopic observation of the wear tracks after pin-on-disc tests as shown in Figure 7: Coatings TiO_2-Cr_2O_3 and n-TiO_2 have wide and deep wear tracks. On the contrary, Cr_2O_3 and n-TiO_2-Cr_2O_3 show small wear scars on the shallow surface, reflecting a mild abrasive wear process for these two coatings.

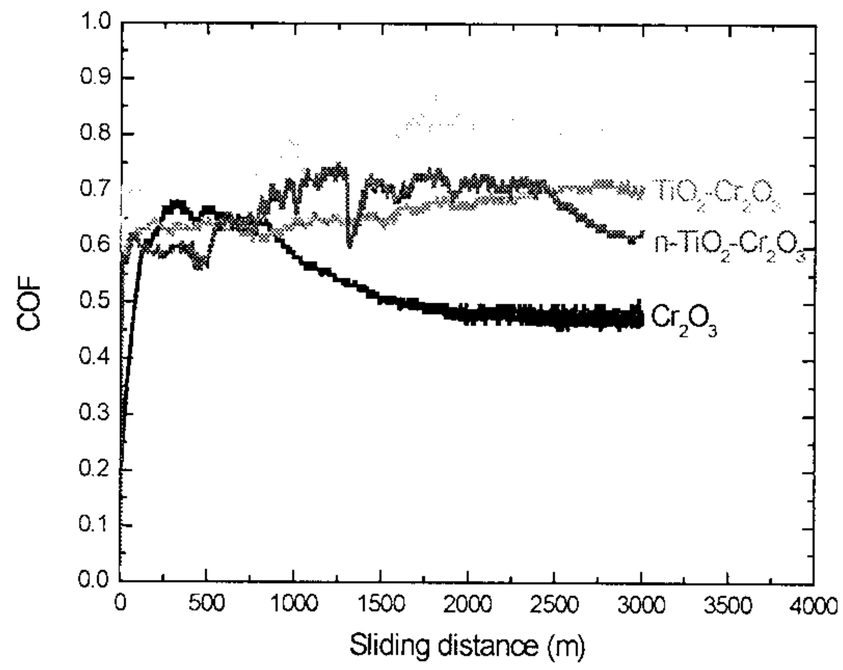


Figure 5: Coefficient of friction vs. sliding distance of different coatings

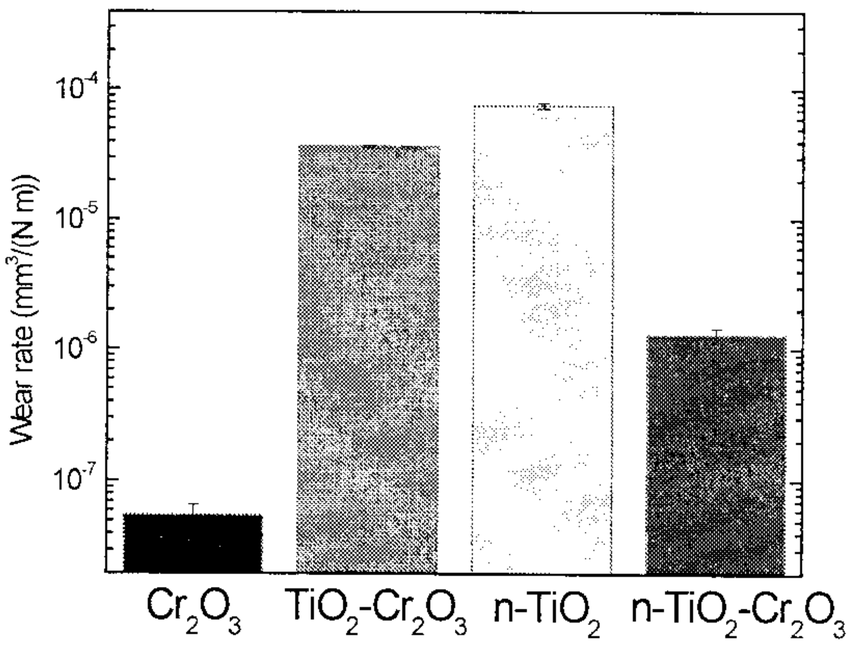
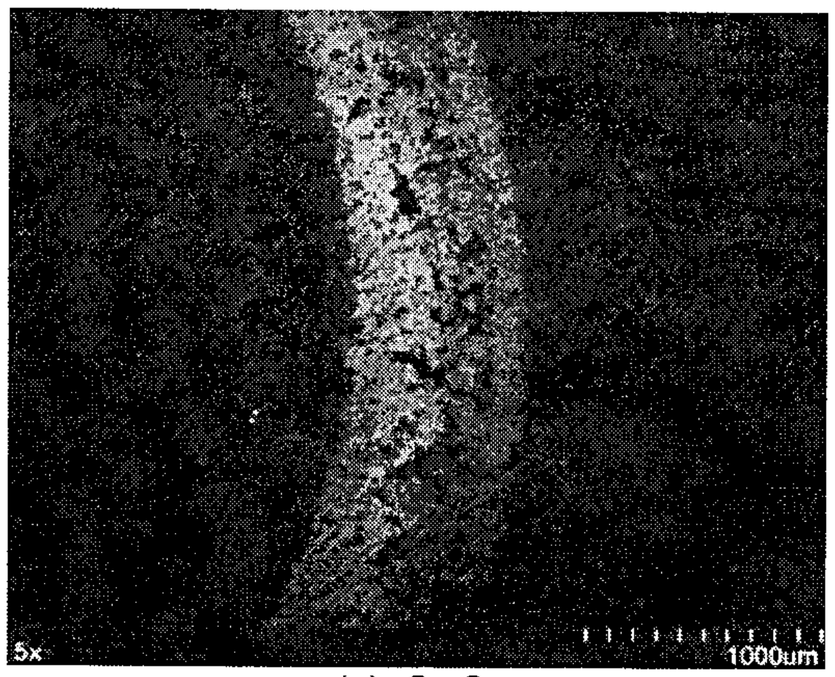
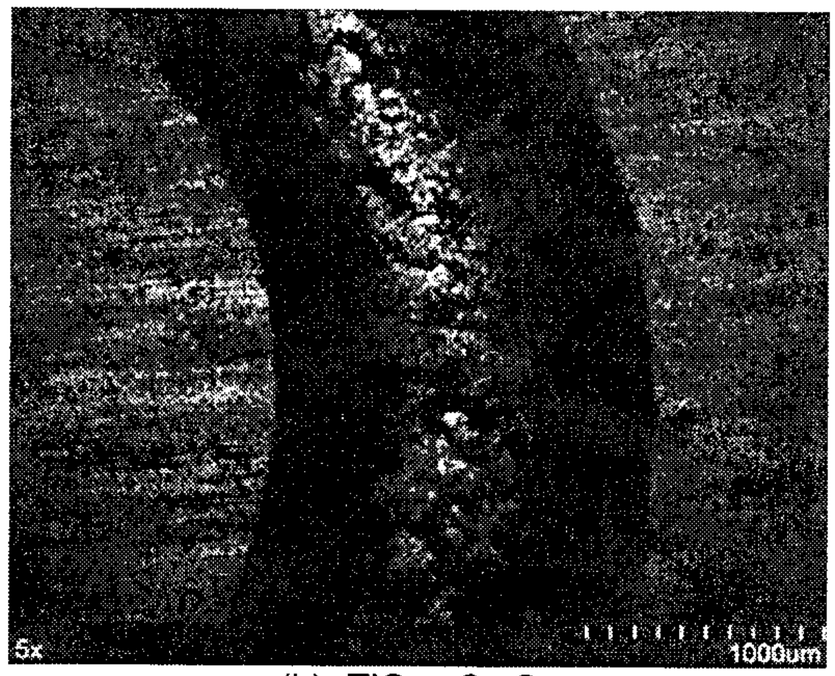


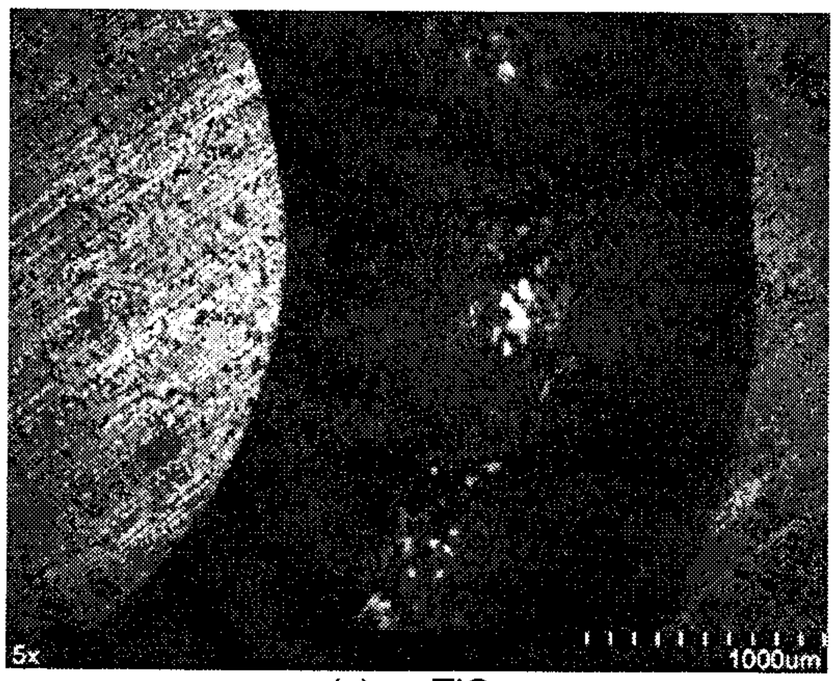
Figure 6: Wear rate of different coatings



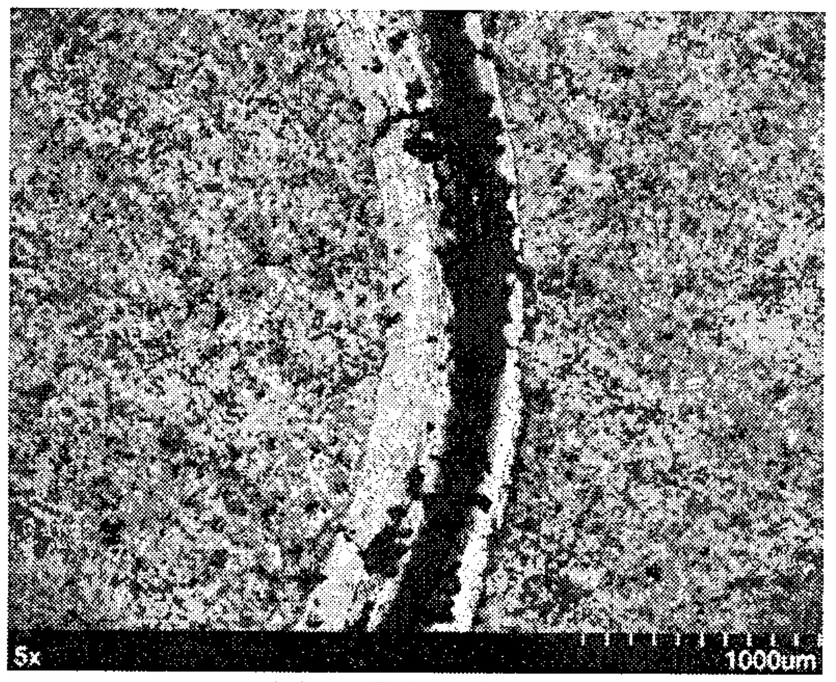
(a) Cr_2O_3



(b) TiO_2 - Cr_2O_3



(c) n-TiO_2



(d) n-TiO_2- Cr_2O_3

Figure 7: Wear tracks after pin-on-disc tests at 50X

Dry Sand Abrasion

From *Table 3*, it is seen that the best dry abrasion wear performance is achieved with the n-TiO_2-Cr_2O_3. This good performance is believed to be due both to the use of the Mettech torch and to combination of n-TiO_2 and Cr_2O_3. It has been shown that the improvement of coating wear performance with n-TiO_2 addition is rather due to an improved coating toughness[5,8].
On the opposite, the poorest wear performance was achieved with the n-TiO_2, which is the coating displaying the lowest hardness. Despite the much higher hardness of the Cr_2O_3, this coating displays average wear performance. This deceptive performance is attributed to Cr_2O_3 brittleness. The wear tracks are shown in *Figure 8*.

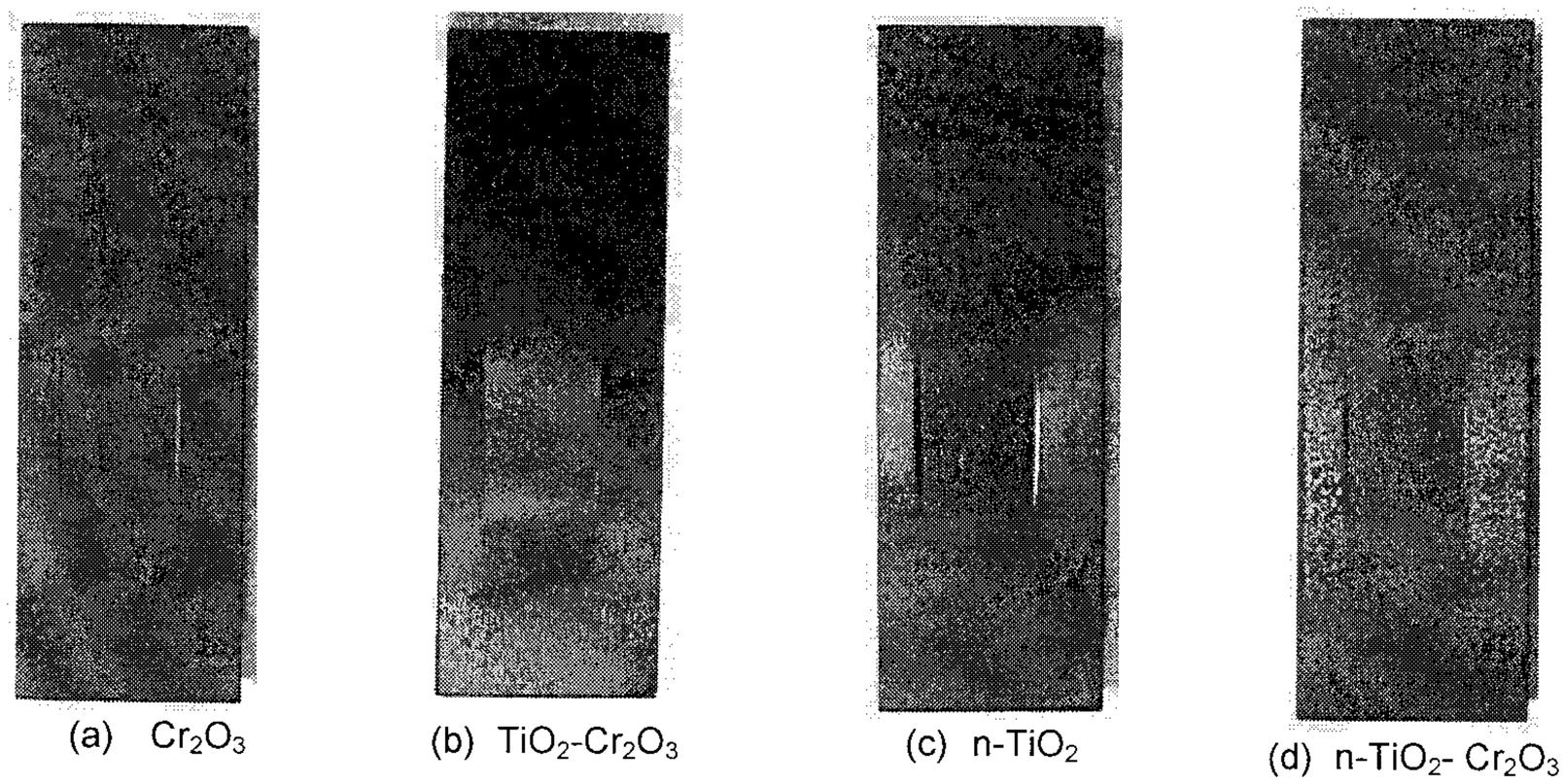


Figure 8: Wear tracks of specimens after dry abrasion test.

Wet Sand Abrasion

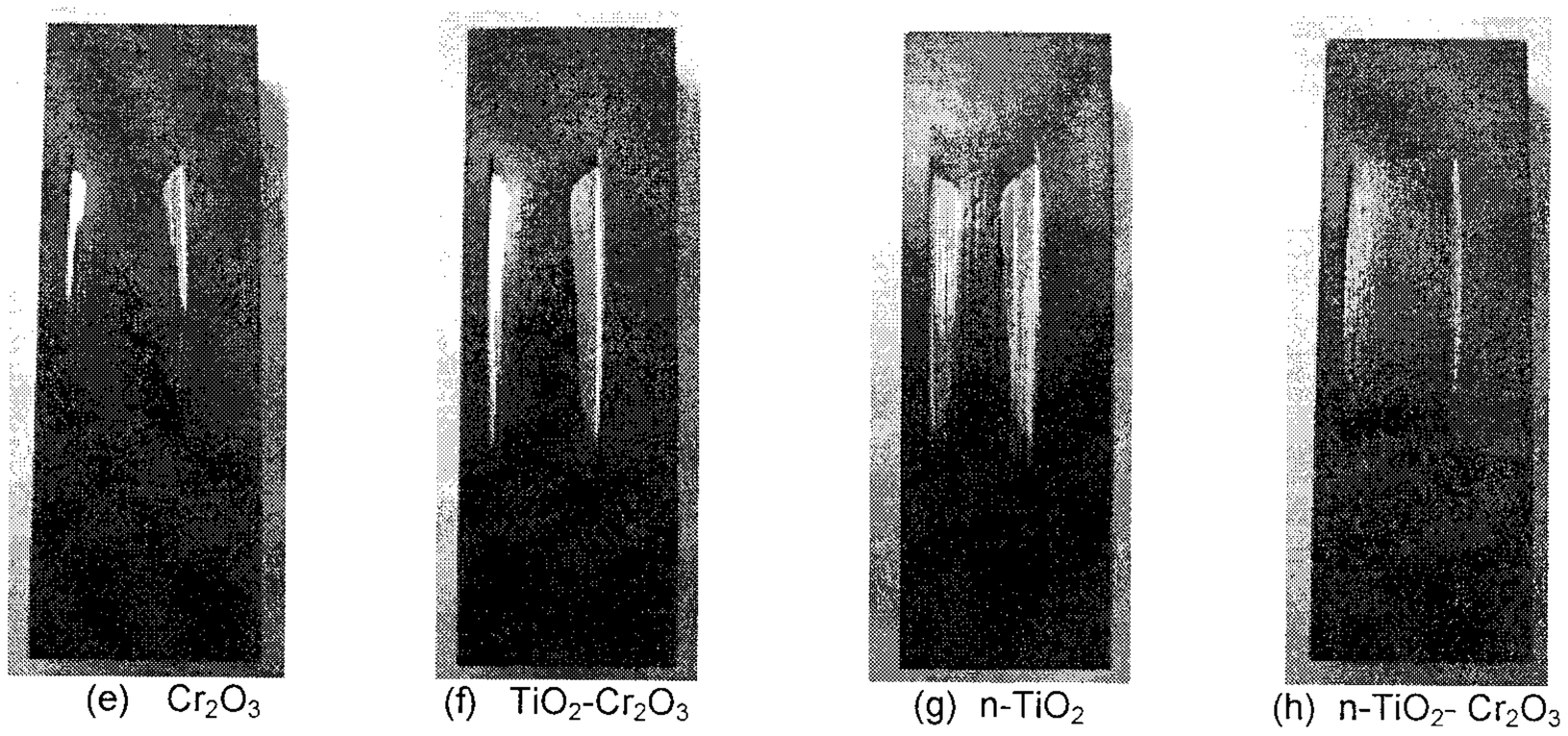


Figure 9: Wear tracks of specimens after wet abrasion test.

From *Figure 9* and in accordance with the dry abrasion results, n-TiO_2-Cr_2O_3 presents the best wet abrasion wear performance and is the only coating that resisted substrate penetration. At the end of the test, n-TiO_2-Cr_2O_3 mass loss was equal to 122.9 mg. Cr_2O_3 coating shows a slight penetration of the substrate while both n-TiO_2 and TiO_2-Cr_2O_3 displayed the poorest performance and the largest penetrations. Tests will be repeated with a revised procedure including a shorter run duration.

Variable Temperature Galling Resistance

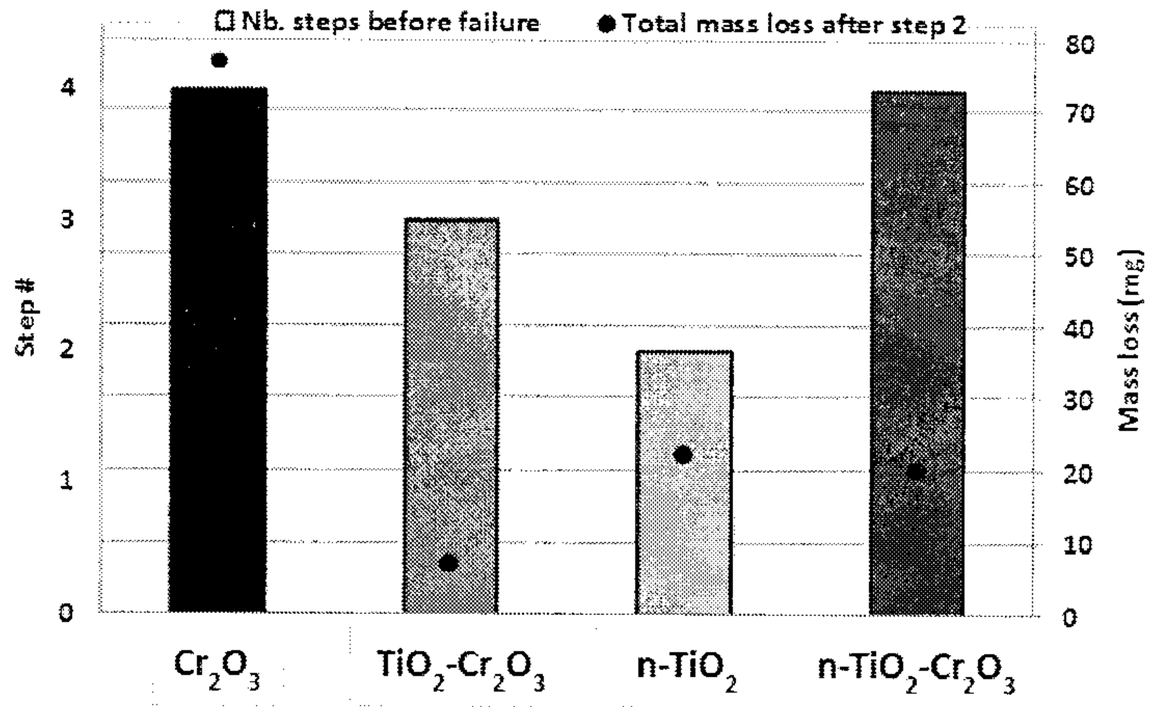
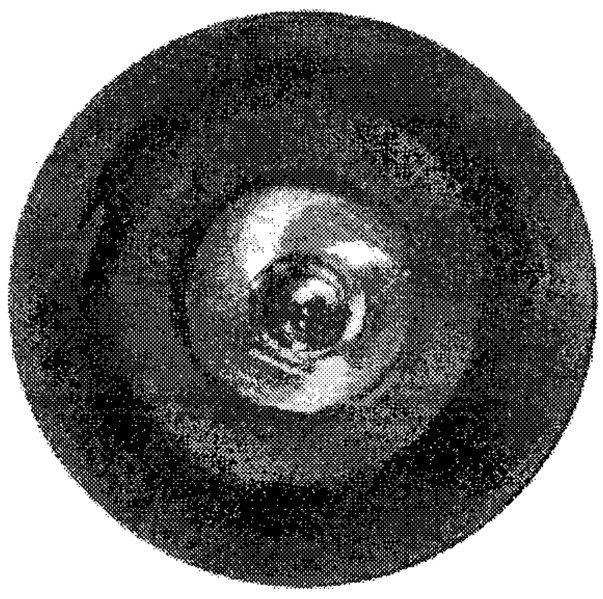
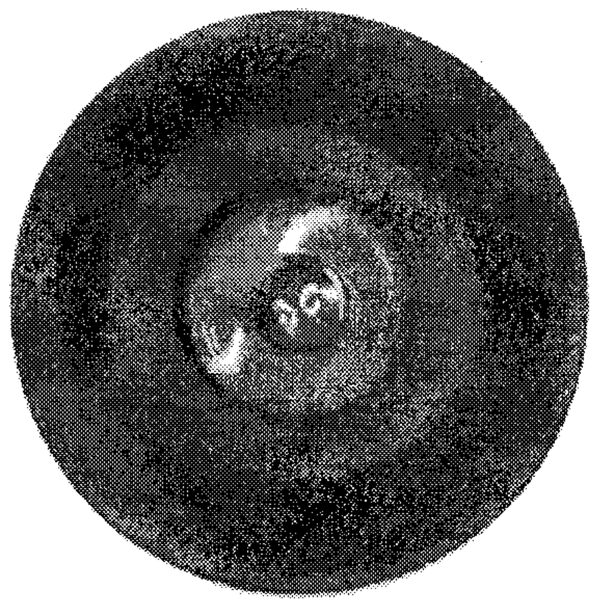


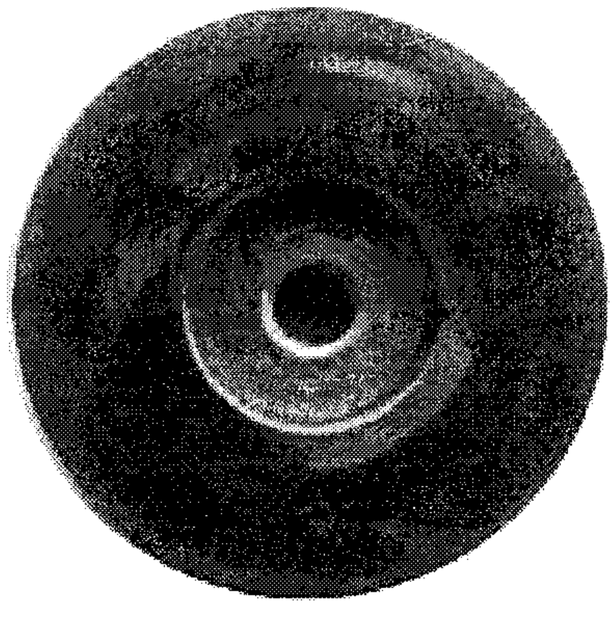
Figure 10: Galling resistance of self-mated specimens after variable temperature galling resistance. Mass loss is given between 0 (initial mass) and 100 cycles (i.e. after step #2)



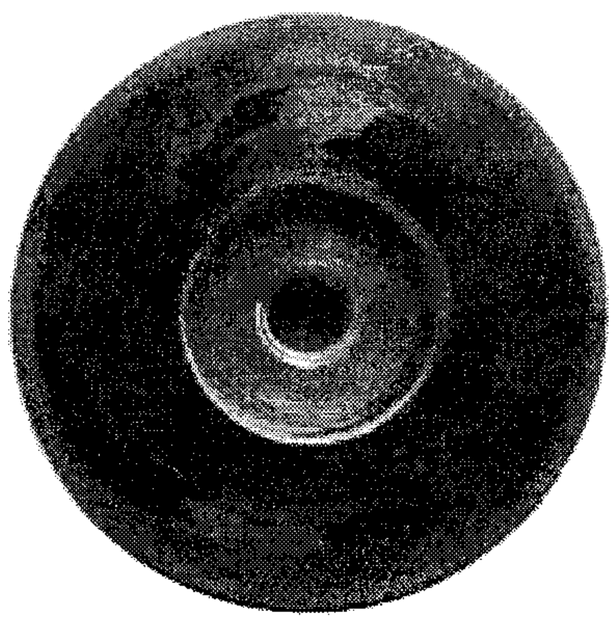
(a) Cr_2O_3 fixed specimen after step 4



(b) Cr_2O_3 rotating specimen after step 4



(c) TiO_2-Cr_2O_3 fixed specimen after step 3



(d) TiO_2-Cr_2O_3 rotating specimen after step 3

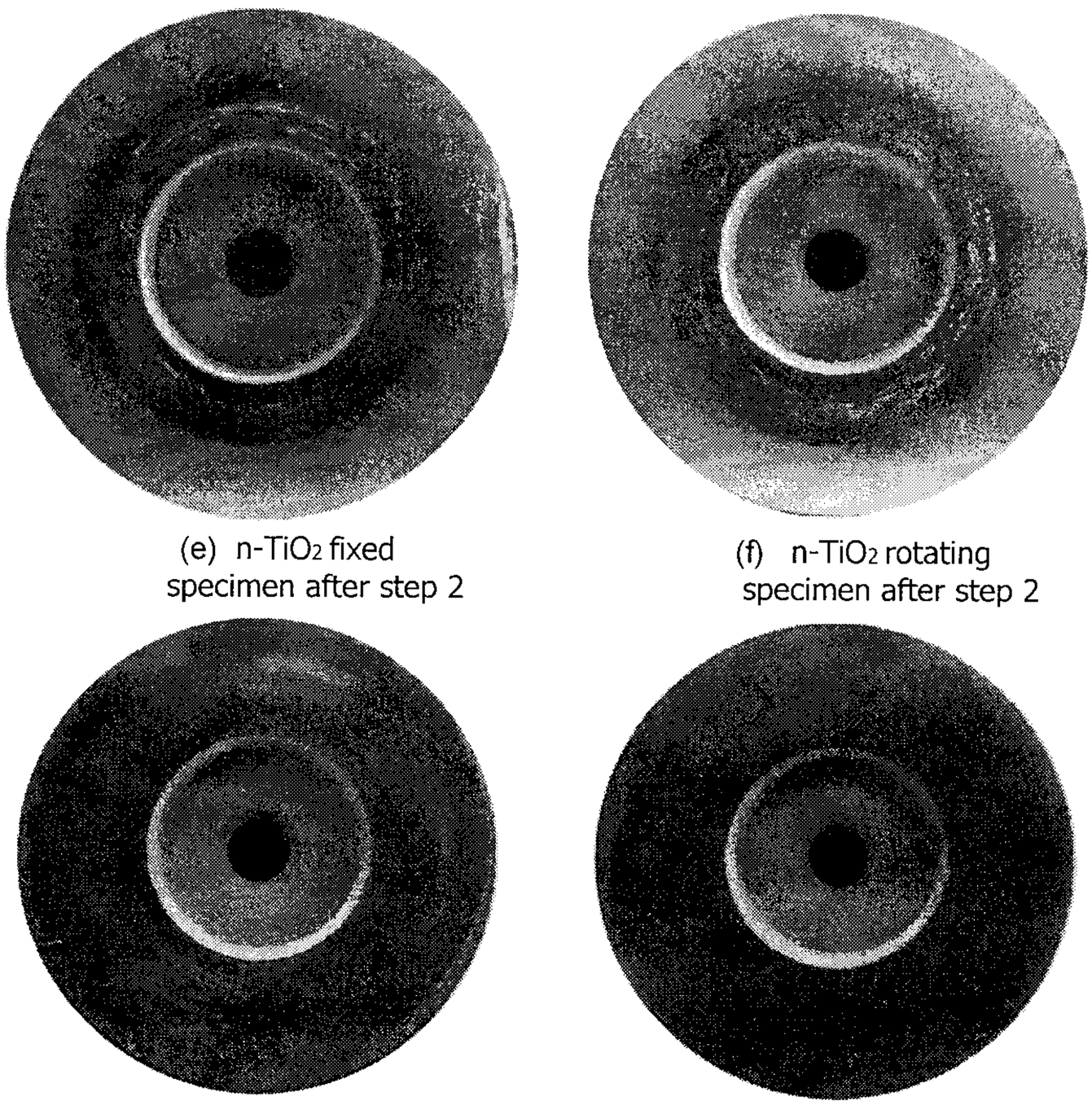


Figure 11: Wear patterns of specimens after variable temperature galling test.

Figure 10 shows the number of steps prior significant wear patterns observation and the total mass loss of the different self-mated specimens (rotating + fixed specimens).. Total mass loss is measured between 0 cycle (initial mass) and 100 cycles (i.e. after step 2). *Figure 11* provides macro-scale pictures of the specimens after the variable temperature galling test. It is demonstrated that Cr_2O_3 (12-a and 12-b) and n-TiO_2-Cr_2O_3 (12-g and 12-h) present the best galling resistance with apparition of light material pick-up and scoring during step #4 (200 cycles run / 220°C / 13.8 MPa). However, Cr_2O_3 mass loss after 100 cycles (77 mg) is approximately four times higher than n-TiO_2-Cr_2O_3 (20 mg). In comparison, both n-TiO_2 (12-e and 12-f) and TiO_2-Cr_2O_3 (12-c and 12-d) combine intermediate galling resistance with low mass loss. They respectively show galling, micro-welding and material pick-up at step #2 (100 cycles run / 220°C / 6.9 MPa) and step #3 (150 cycles run / 220°C / 10.3 MPa) while their mass loss stay below 22 mg after 100 cycles. It is assumed that Cr_2O_3 high mass loss in comparison to other specimens is mainly due to its brittleness. By achieving the highest number of steps prior significant wear patterns observation and by exhibiting a low mass loss, n-TiO_2-Cr_2O_3 ranks 1st. Cr_2O_3, TiO_2-Cr_2O_3, n-TiO_2 are respectively ranked 2nd, 3rd and 4th.

CONCLUSIONS

In this study, the load carrying capacity and the tribological resistances of 4 ceramic coatings potentially suitable for HPAL have been evaluated.

Pure Cr_2O_3 blend has shown the highest hardness and best sliding wear resistance and COF while the n-TiO_2 has demonstrated the lowest hardness, the poorest wear rate and the highest COF. As predicted by the intuition, Cr_2O_3-TiO_2 and n-TiO_2-Cr_2O_3 blends have offered hardness and sliding measurements in between the measurements of each pure ceramics in its composition.

When looking at abrasion, our study shows positive and counter intuitive results. n-TiO_2-Cr_2O_3 blends has obtained superior resistance for both dry and wet abrasion test compare to other pure ceramics. According to a study published by Velan, the high performance of the TiO_2-Cr_2O_3 has been attributed to the optimized balance between the hard and brittle Cr_2O_3 phases and the soft and ductile TiO_2 phases. The current paper shows how the synergy between those two materials yields to abrasion performances exceeding the one of each individual.

When looking at galling, n-TiO_2-Cr_2O_3 ranks 1st by achieving the highest number of steps prior significant wear patterns observation and by exhibiting low mass loss. Cr_2O_3 , TiO_2-Cr_2O_3 and n-TiO_2 are respectively ranked 2nd, 3rd and 4th.

Promisingly, the novel mix of n-TiO_2 and Cr_2O_3 has systematically offered better tribological performance than Velan proprietary TiO_2-Cr_2O_3 blend. Consequently this novel blend appears as a promising evolution of the current TiO_2-Cr_2O_3 blend. Further optimization is needed to commercialize use.

Works is still needed to optimize surface preparation, spraying procedure and post-treatment for the novel mix of Cr_2O_3 and n-TiO_2 in order to achieve equivalent or better results than current TiO_2-Cr_2O_3 blend, especially regarding bond and shear strength. Indeed, current Cr_2O_3-TiO_2 has displayed the highest bond and shear strength compare to all other materials, including the nano-coatings. Developing an HVOF process capable of spraying TiO_2-Cr_2O_3 could be an interesting process to achieve these results. The challenge for such development is to ensure melting of the Cr_2O_3 particles in order to avoid the rebound of those particles when impacting the substrate as well as the erosion of the deposited TiO_2 layer by the same particles.

Works is also needed to secure supply chain and develop quality standard for this novel material in order to avoid production delays and / or quality issues. Furthermore corrosion tests will be required to fully assess material corrosion performance.

In the mean time, in view of those recent results, TiO_2-Cr_2O_3 offers the best overall tribological performance compare to other tested ceramics, namely Cr_2O_3 and n-TiO_2.

ACKNOWLEDGEMENTS

The authors wish to thank Mr. Rabih Matar (Velan), Jean-Claude Tremblay (NRC), Michel Thibodeau (NRC) and David De Lagrave (NRC) for their technical support as well as David Lee (Kennametal Stellite) for useful discussion. Finally, we greatly appreciate Velan's interest and support of this research.

REFERENCES

1. L. Leblanc, *et al.*, "High Performance Coatings for Severe Service Ball Valves in HPAL: Development and Field Results," presented at the ALTA, 2008.

2. G. E. Kim, *et al.*, "Thermal spray coatings for ball valves used in Nickel/Cobalt pressure acid leaching," in *International Spray Show Conference*, Montreal, Canada, 2000, pp. 1149-1153.

3. J. Williams, *et al.*, "Ball valves with nanostructured titanium oxide coatings for high-pressure acid-leach service: development to application," in *Pressure Hydrometallurgy*, Banff, Canada, 2004, pp. 663-681.

4. G. Kim and J. Walker, "Successful Application of Nanostructured Titanium Dioxide Coating for High-Pressure Acid-Leach Application," *Journal of Thermal Spray Technology,* vol. 16, pp. 34-39, 2007.

5. R. S. Lima, *et al.*, "Abrasion behaviour of nanostructured and conventional titania coatings thermally sprayed via APS, VPS and HVOF," in *International Thermal Spray 2004 Conference*, Osaka, Japan, 2004.

6. P. Ctibor and M. Hrabovsky, "Plasma sprayed TiO_2: The influence of power of an electric supply on particle parameters in the flight and character of sprayed coating," *Journal of the European Ceramic Society,* vol. 30, pp. 3131-3136, 2010.

7. D. J. Greving, *et al.*, "Effects of coating thickness and residual stresses on the bond strength of ASTM C633-79 thermal spray coating test specimens," *Journal of Thermal Spray Technology,* vol. 3, pp. 371-378, 1994.

8. L. T. Kabacoff, "Nanoceramic Coatings Exhibit Much Higher Toughness and Wear Resistance than Conventional Coatings," *The AMPTIAC Newsletter,* vol. 6, pp. 37-42, 2002.

CLAIMS

1. A method for depositing a ceramic coating on a substrate, the method comprising:

    - mixing a powder of sprayable nanostructured titanium(IV) oxide (n-TiO_2) and a powder of chromium(III) oxide (Cr_2O_3), thereby obtaining a n-TiO_2-Cr_2O_3 powder blend; and

    - thermal spraying particles of the n-TiO_2-Cr_2O_3 powder blend on the substrate at an in-flight particle temperature greater than 2350°C and a particle in-flight velocity greater than 350 m/s, thereby obtaining a coated substrate.

2. The method of claim 1, wherein the substrate is a metal substrate.

3. The method of claim 2, wherein the metal substrate comprises one of titanium, a titanium alloy, stainless steel, steel, a high-performance nickel alloy, a high-performance cobalt alloy, bronze and a copper alloy.

4. The method of claim 3, wherein the metal substrate comprises one of titanium and stainless steel.

5. The method of any one of claims 1 to 4, wherein the powder of sprayable n-TiO_2 comprises nanosized constituents agglomerated and/or sintered in microsized n-TiO_2 particles.

6. The method of claim 5, wherein the nanosized constituents have a size ranging from 50 nm to 200 nm.

7. The method of claim 5 or 6, wherein the microsized n-TiO_2 particles have a diameter distribution ranging from 4 µm to 100 µm.

8. The method of any one of claims 1 to 7, wherein the n-TiO_2-Cr_2O_3 powder blend comprises 40 wt% to 70 wt% of n-TiO_2 and 30 wt% to 60 wt% of Cr_2O_3.

9. The method of claim 8, wherein the n-TiO_2-Cr_2O_3 blend comprises 50 wt% to 60 wt% of n-TiO_2 and 40 wt% to 50 wt% of Cr_2O_3.

10. The method of claim 8, wherein the n-TiO_2-Cr_2O_3 blend comprises 53 wt% to 57 wt% of n-TiO_2 and 43 wt% to 47 wt% of Cr_2O_3.

11. The method of claim 8, wherein the n-TiO_2-Cr_2O_3 blend comprises about 55 wt% of n-TiO_2 and about 45 wt% of Cr_2O_3.

12. The method of any one of claims 1 to 11, wherein the thermal spraying is air plasma spraying (APS).

13. The method of any one of claims 1 to 12, wherein the in-flight particle temperature is greater than 2350°C up to 2800°C.

14. The method of claim 13, wherein the in-flight particle temperature is from 2400°C to 2800°C.

15. The method of claim 13, wherein the in-flight particle temperature is from 2500°C to 2800°C.

16. The method of claim 13, wherein the in-flight particle temperature is about 2590°C.

17. The method of any one of claims 1 to 16, wherein the particle in-flight velocity is greater than 400 m/s.

18. The method of claim 17, wherein the particle in-flight velocity is greater than 450 m/s.

19. The method of claim 18, wherein the particle in-flight velocity is about 457 m/s.

20. A substrate coated with a nanostructured titanium(IV) oxide- chromium(III) oxide (n-TiO_2-Cr_2O_3) coating, the coating having a microhardness of at least 1000 HV and a dry abrasion volume loss of less than 15 mm^3 .

21. The substrate of claim 20, wherein the microhardness is of at least 1150 HV.

22. The substrate of claim 20 or 21, wherein the dry abrasion loss is less than 8.4 mm^3.

23. The substrate of any one of claims 20 to 22, wherein the microhardness is between 1150 and 1250 HV and the dry abrasion loss is between 7 and 8.4 mm^3.

24. The substrate of any one of claims 20 to 23, wherein the n-TiO_2-Cr_2O_3 coating comprises 40 wt% to 70 wt% of n-TiO_2 and 30 wt% to 60 wt% of Cr_2O_3.

25. The substrate of any one of claims 20 to 24, wherein the n-TiO_2-Cr_2O_3 coating comprises 50 wt% to 60 wt% of n-TiO_2 and 40 wt% to 50 wt% of Cr_2O_3.

26. The substrate of any one of claims 20 to 25, wherein the n-TiO_2-Cr_2O_3 coating comprises 53 wt% to 57 wt% of n-TiO_2 and 43 wt% to 47 wt% of Cr_2O_3.

27. The substrate of any one of claims 20 to 26, wherein the n-TiO_2-Cr_2O_3 coating comprises about 55wt% of n-TiO_2 and about 45wt% of Cr_2O_3.

28. The substrate of any one of claims 20 to 27, wherein the substrate is a mechanical part.

29. The substrate of claim 28, wherein the mechanical part is a valve element of a valve.

30. The substrate of claim 29, wherein the valve element is a ball valve element.

31. A mechanical part coated with a ceramic coating, wherein the ceramic coating is deposited using the method of any one of claims 1 to 19.

NANOSTRUCTURED AND CONVENTIONAL Cr_2O_3, TiO_2 AND TiO_2-Cr_2O_3 THERMAL SPRAYED COATINGS FOR METAL SEATED BALL VALVE APPLICATIONS IN HYDROMETALLURGY

Luc Vernhes, Craig Bekins, Nicolas Lourdel
Velan, Canada

Dominique Poirier, Rogerio S. Lima
National Research Council of Canada (NRC), Canada

Duanjie Li, Jolanta E. Klemberg-Sapieha
Polytechnique Montréal, Canada

ALTA 2013
25 May - 1 June
Perth, Western Australia

OUTLINE

- BACKGROUND
- STUDY OBJECTIVES
- EXPERIMENTAL PROCEDURES & RESULTS
  - Microstructure
  - Mechanical Properties
    1) Microhardness
    2) Bond Strength (Shear)
  - Tribological Performance
    1) Sliding Wear
    2) Dry Sand Abrasion
    3) Wet Sand Abrasion
    4) Variable Temperature Galling
- CONCLUSION

BACKGROUND

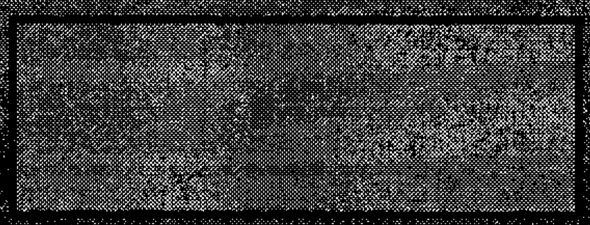
- COATINGS ARE APPLIED TO PROTECT SURFACES
- THERE IS NO "ONE SIZE FITS ALL" COATING
- OPTIMIZING COATINGS INCREASES LIFE



BACKGROUND

To improve the properties of the surface while leaving the bulk material intact

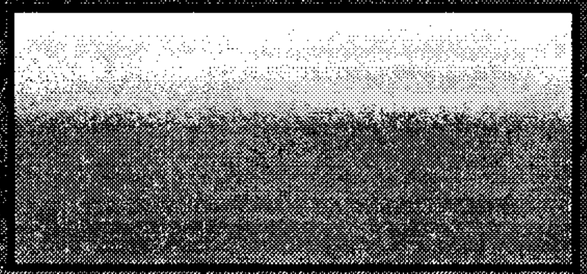
Bare material



Coating



Surface modification



Modified surface + coating (duplex)



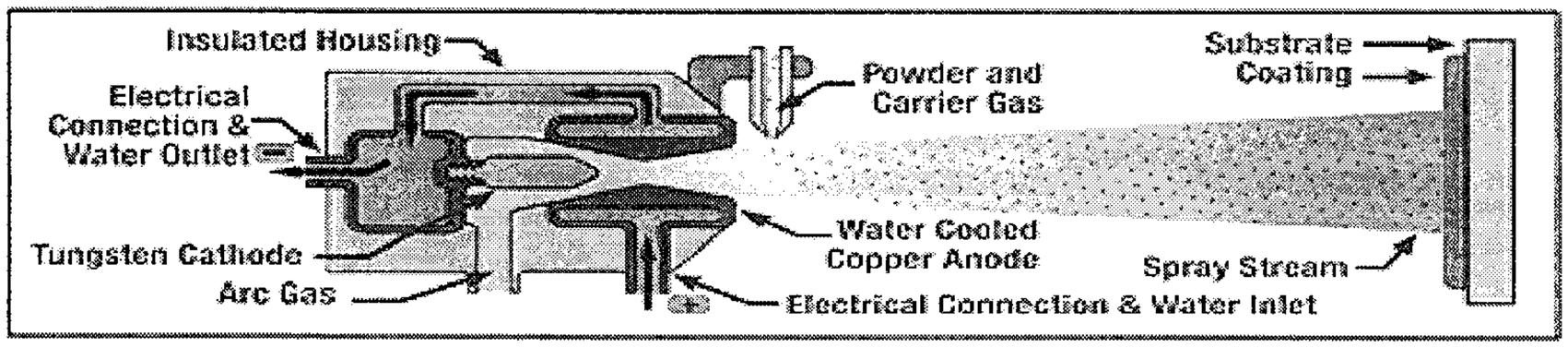
BACKGROUND

Coating	**Weld Overlay** *MIG, TIG, PTA, Laser*	•Stainless •Cobalt Alloy (Stellite®) •Nickel Alloy (Inconel®)
	Plating *Electroplating, Chemical*	•Chrome •Nickel
	Thermal Spray *HVOF, Plasma*	•*Cermet : Cr_3C_2-NiCr, WC-CoCr, $(W,Cr)C_x$-Ni* •*Ceramic : Cr_3O_2, TiO_2, TiO_2-Cr_2O_3* •*Metal : Aluminum, Nickel Alloy, Cobalt Alloy*
	Brazing / Fusing *S&F, Conformaclad, Ultraflex*	•*Co- and Ni-based alloys (NiCrB, Metco 19E, C88)* •*Carbide Blends (WC and Cr_3C_2)*
	Thin Film *CVD, PVD*	•*Tungsten/Tungsten Carbide (Hardide®)* •*Diamond Like Carbon (DLC)* •*Tantalum (Tantaline®)*
Surface modification	**Diffusion** *Salt Bath, Gas, Plasma*	•*Nitriding, Boriding, Chromizing, Carburizing* •*Quench Polish Quench (QPQ nitrocarburizing)*
	Microstructure	•*Superficial Heat Treatment : Induction, Flame, Laser* •*Mechanical : Sand-blasting, Shot peening*

BACKGROUND

- AIR PLASMA SPRAY
  - Generates an inert plasma gas (clean – no unburned residue),
  - Very high temperatures (ideal for ceramics),
  - High cost but incredible versatility
  - Velan uses this process to deposit ceramics required for abrasive and corrosive applications (POx and HPAL)
    - Cr_2O_3
    - TiO_2
    - TiO_2-Cr_2O_3

Plasma Spray Process



Characteristics

Flame Temperature:
Approximately 12,000 - 20,000 °F (6,000 - 11,100 °C)

Gases Used:
Ar/H_2
$N2/H_2$

Particle Speed:
800 - 1,900 ft/s (240-550 m/s)

Photo Courtesy of Westaim Ambeon

BACKGROUND

HYDROMETALLURGY PROJECTS *CHRONOLOGICAL ORDER*	PROCESS	VELAN EXPERIENCED THERMAL SPRAY COATINGS
Nerco's Con	POx	Cr_2O_3
Barrick	POx	Cr_2O_3
Lone Tree	POx	Cr_2O_3
Lihir	POx	Cr_2O_3
Porgera	POx	Cr_2O_3
Falconbridge	HPAL - pilot plant	Cr_2O_3, TiO_2, TiO_2-Cr_2O_3 & others
Cawse	HPAL	TiO_2-Cr_2O_3
Murin-Murin	HPAL	TiO_2-Cr_2O_3
Coral Bay	HPAL	TiO_2-Cr_2O_3
Goro	HPAL	TiO_2-Cr_2O_3
Ambatovy	HPAL	TiO_2-Cr_2O_3
Taganito	HPAL	TiO_2-Cr_2O_3

- The HPal Falconbridge project has faced Cr_2O_3 failure due to corrosion mechanism
- After testing several solutions, the new TiO_2-Cr_2O_3 coating was successfully launched Coating contains TiO_2 and Cr_2O_3 in order to get the corrosion resistance of a pure TiO_2 and the tribological performances of Cr_2O_3

OBJECTIVES

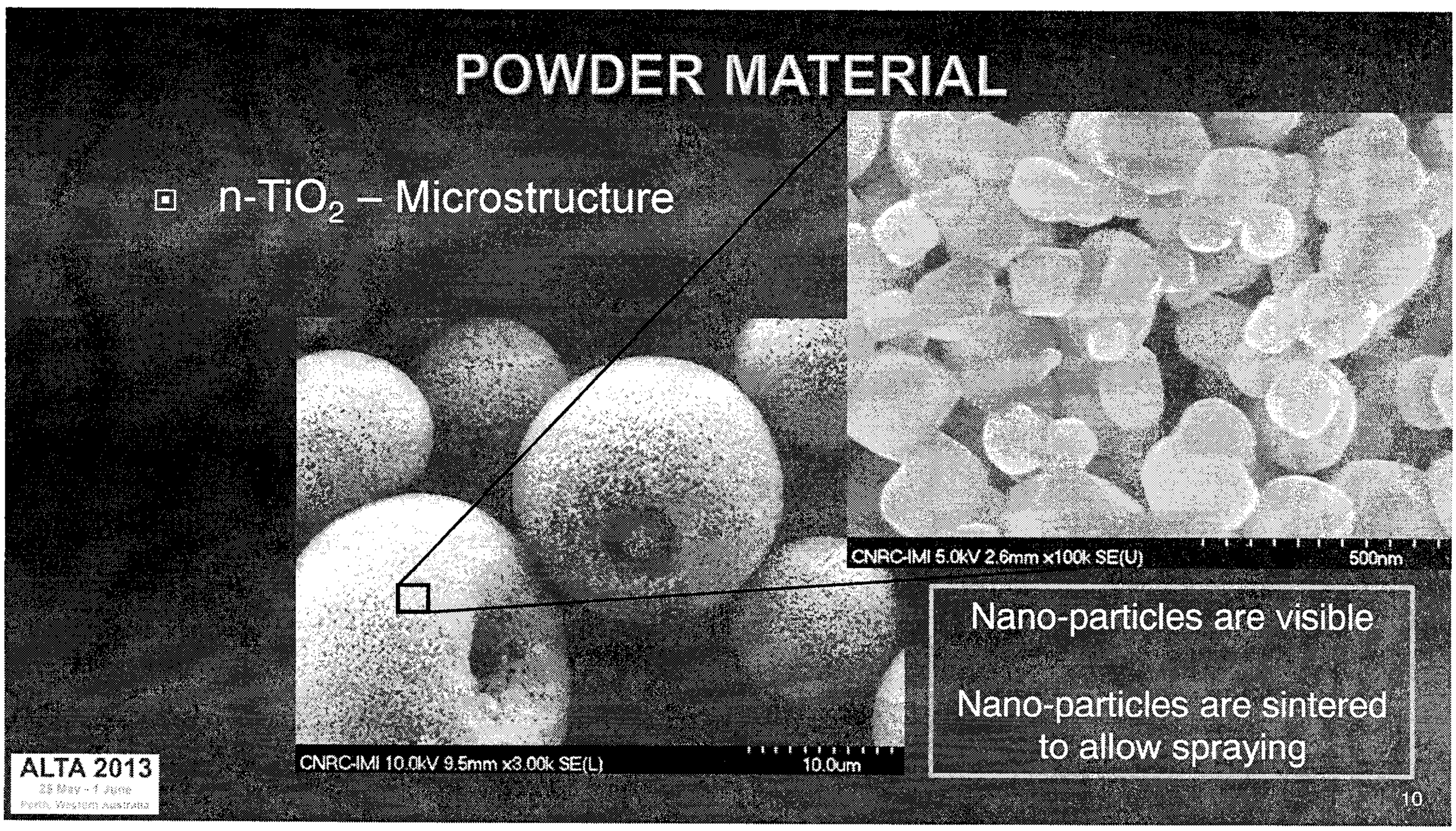
- To characterize n-TiO_2 deposited by APS (NRC technology),
- To develop and to characterize novel n-TiO_2-Cr_2O_3 coating deposited by APS (NRC + Velan technology),
- To compare their performance with Velan current Cr_2O_3 and TiO_2-Cr_2O_3 coatings.

EXPERIMENTAL

- 4 coatings tested:
  - Cr_2O_3 (Velan proprietary blend)
  - TiO_2-Cr_2O_3 (Velan proprietary blend)
  - n-TiO_2 (Millydine supplier)
  - n-TiO_2-Cr_2O_3 (Velan proprietary blend - **NOVEL**)
- Coatings applied onto titanium coupons
  - Previously grit blasted (Al_2O_3 - grit 24)
- Nominal coating thickness of 0.020" (500 µm)

POWDER MATERIAL

- *n*-TiO_2 – Microstructure

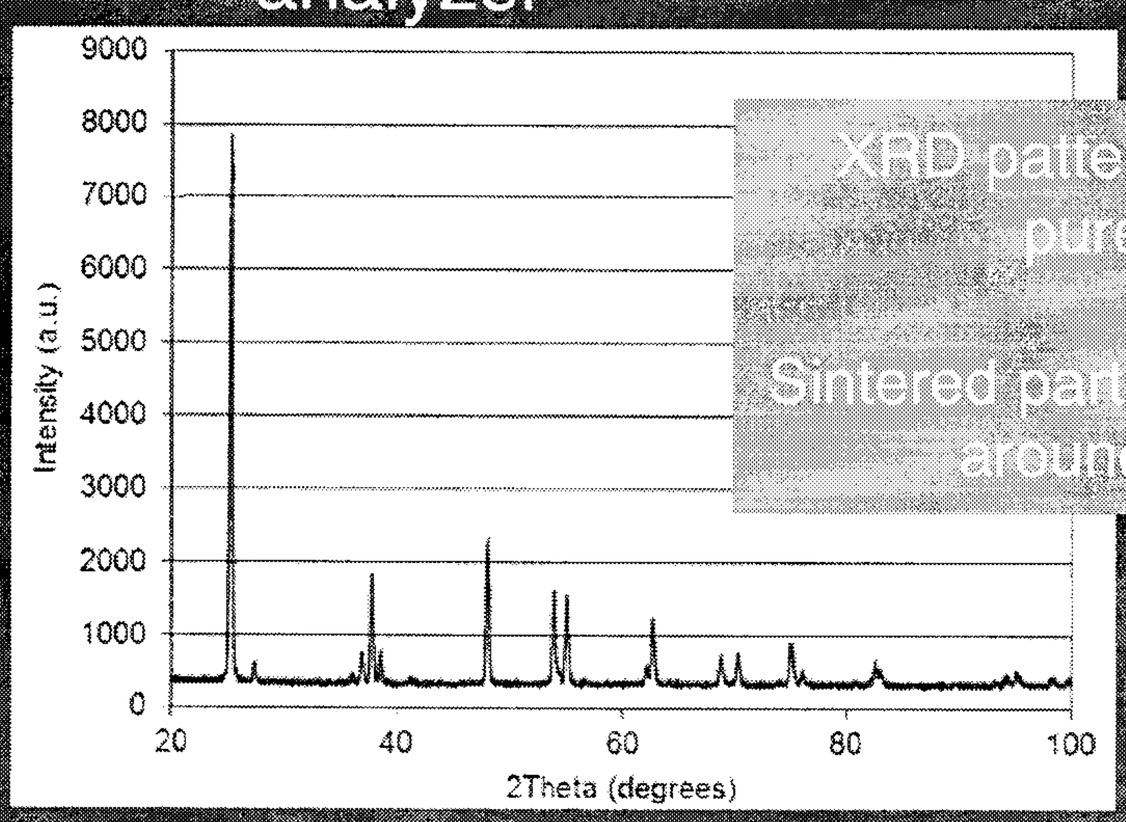


Nano-particles are visible

Nano-particles are sintered to allow spraying

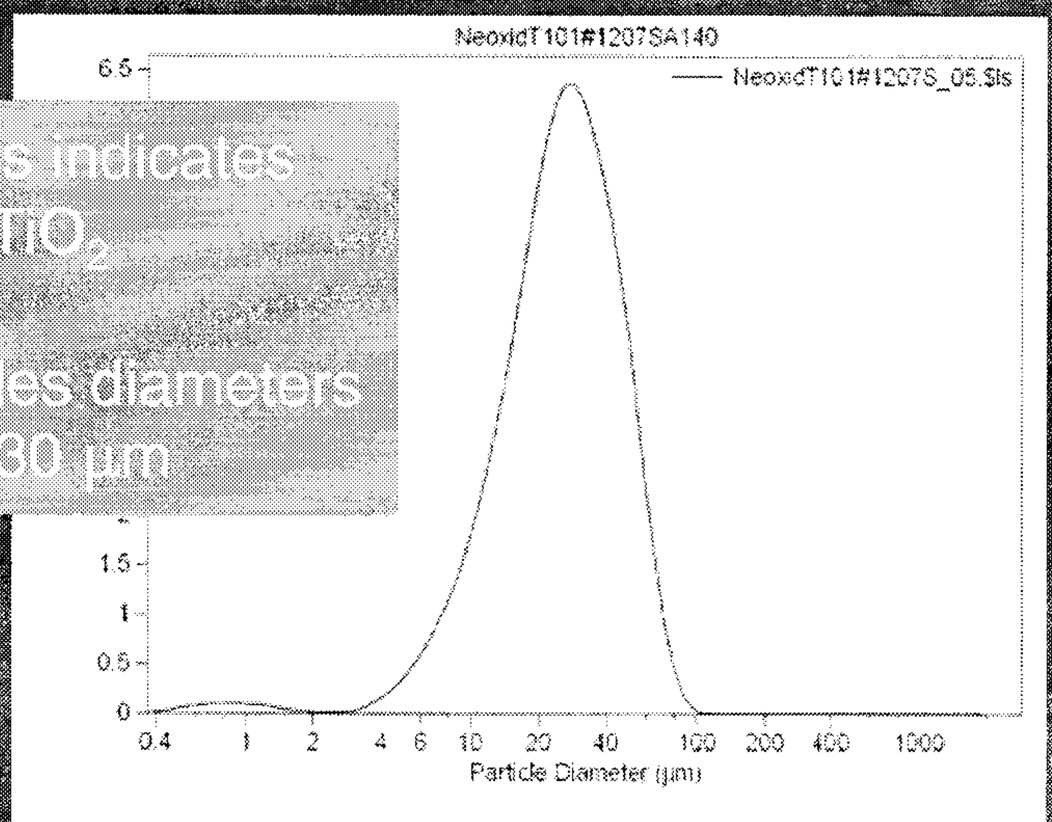
POWDER MATERIAL

- n-TiO_2 – X-Ray Diffraction and laser diffraction particle size analyzer



XRD patterns indicates pure TiO_2

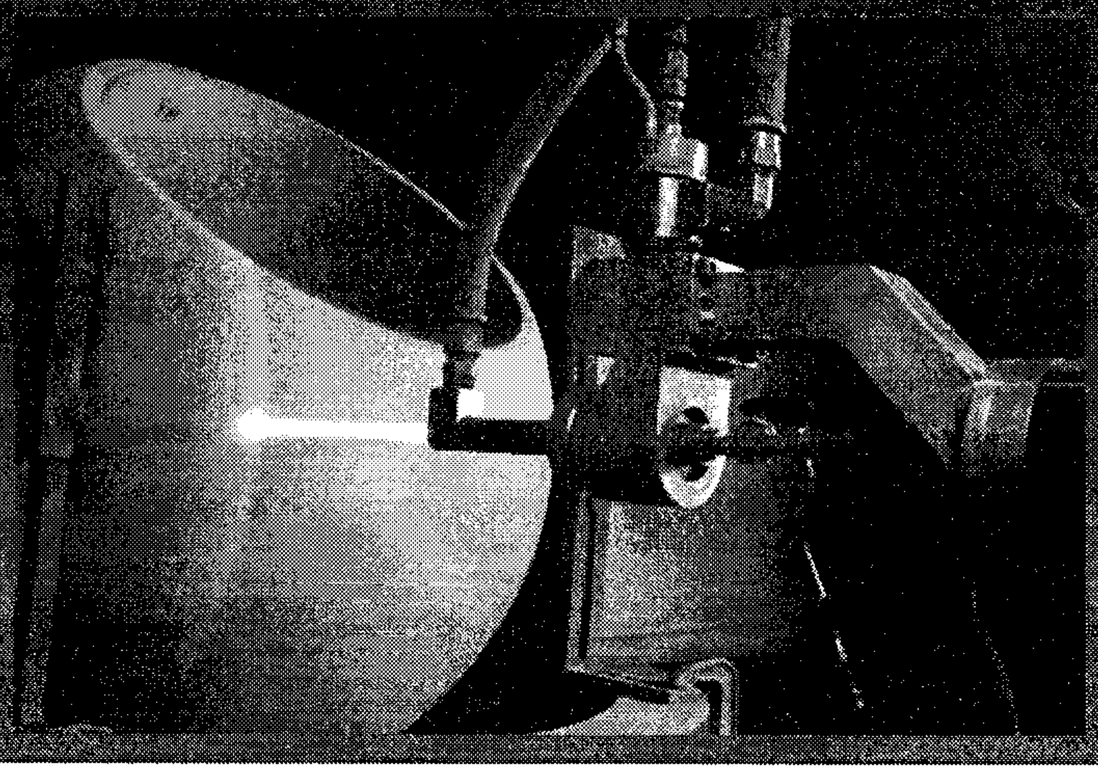
Sintered particles diameters around 30 µm



ALTA 2013
28 May - 1 June
Perth, Western Australia

POWDER MATERIAL

- Novel blend of n-TiO_2 and Cr_2O_3
  - n-TiO_2 powder from Millydine mixed with Metco 106, which is a fused, sintered and crushed Cr_2O_3 powder,
  - Mettech Axial III APS torch.



POWDER MATERIAL

	Cr_2O_3	TiO_2-Cr_2O_3	n-TiO_2	n-TiO_2-Cr_2O_3
Torch	SG-100	SG-100	Mettech Axial III	Mettech Axial III
Ar flow (lpm)	53	53	37.5	62.5
H_2 flow (lpm)	*Confidential*		37.5	62.5
N_2/He flow (lpm)	41 He	41 He	75 N_2	125 N_2
Current (A)	800	800	3 x 230	3 x 230
Voltage (V)	~ 42	~ 42	152	205
Power (kW)	33.6	33.6	105	141
Net Power (kW) or Enthalpy (kJ/L)	*Confidential*		15.0 kJ/L	18.2 kJ/L
Nozzle	730 Anode / 129 Cathode	730 Anode / 129 Cathode	3/8"	3/8"
Spraying Distance (cm)	6.35	6.35	14	14
Feedrate (g/min)	~ 30	~ 30	18	18
Ar Carrier Gas (lpm)	5	5	9	9
In-flight Temperature (°C)	*Confidential*		2578±166	2590±258
In-flight Velocity (m/s)			269±45	457±91

3 electrodes provide high power

Min. in-flight temperature just above Cr_2O_3 melting point (2,350°C)

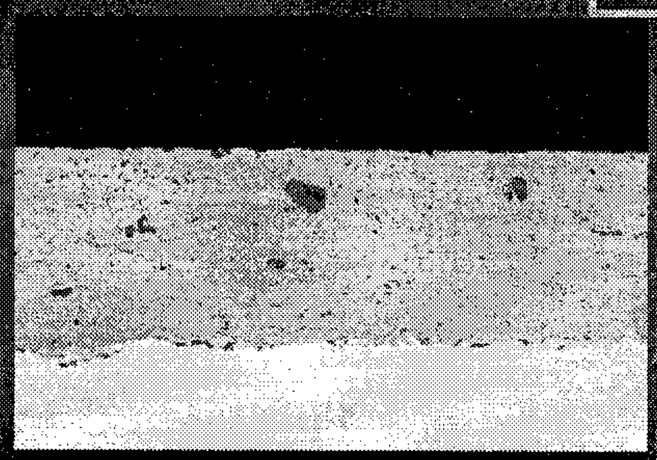
Based on a separate study, nano particles are preserved

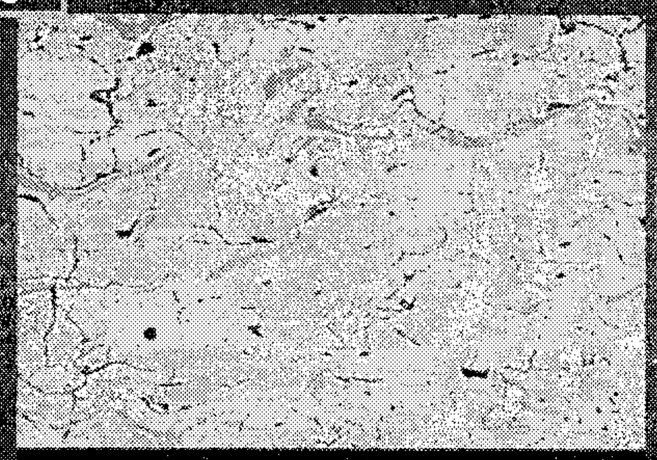
MICROSTRUCTURE

All coatings have shown low levels of porosity

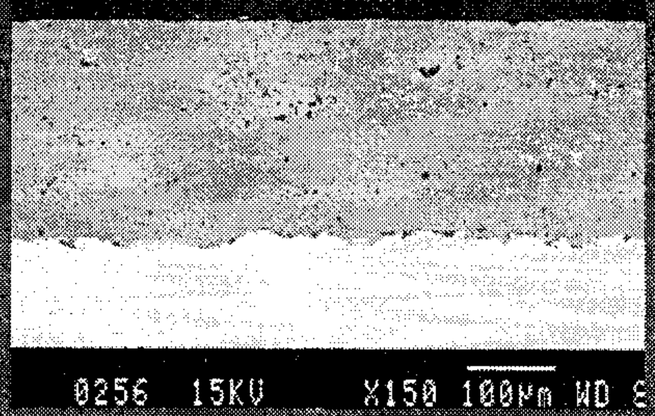
Two phases present in the coatings with the blend powder feedstock are Cr_2O_3 (light grey) and TiO_2 (dark grey) respectively

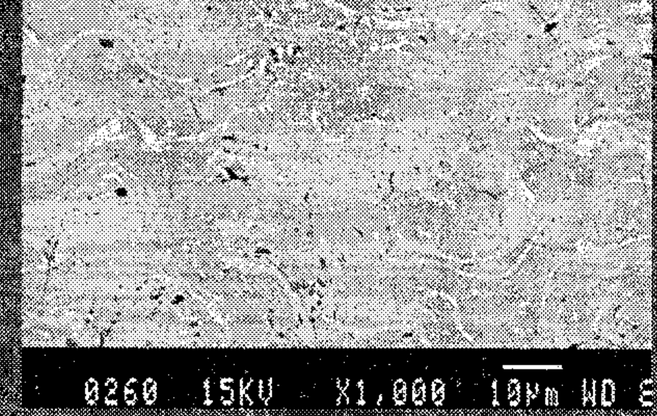
Cr_2O_3





TiO_2-Cr_2O_3



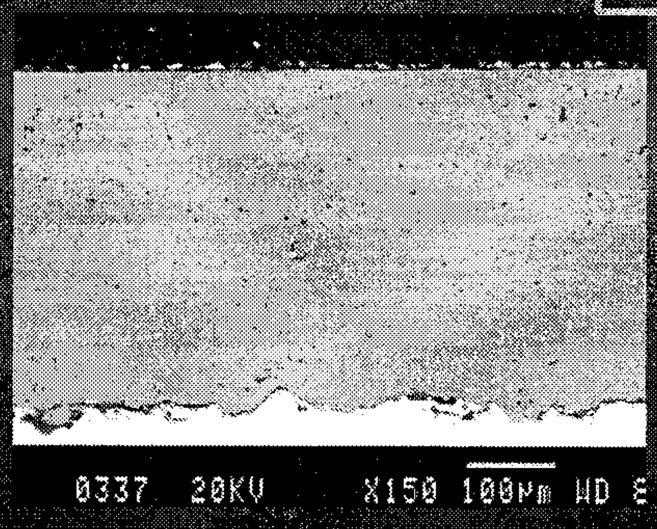


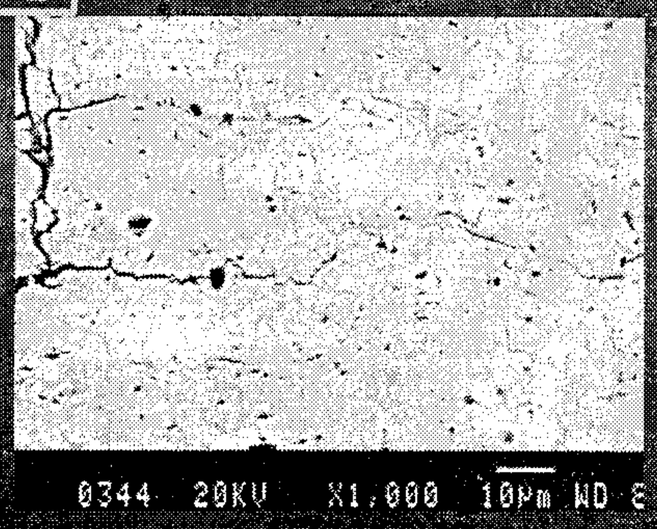
MICROSTRUCTURE

Fine cracks seen in particles and at particle boundaries are thought to be formed due to quenching.

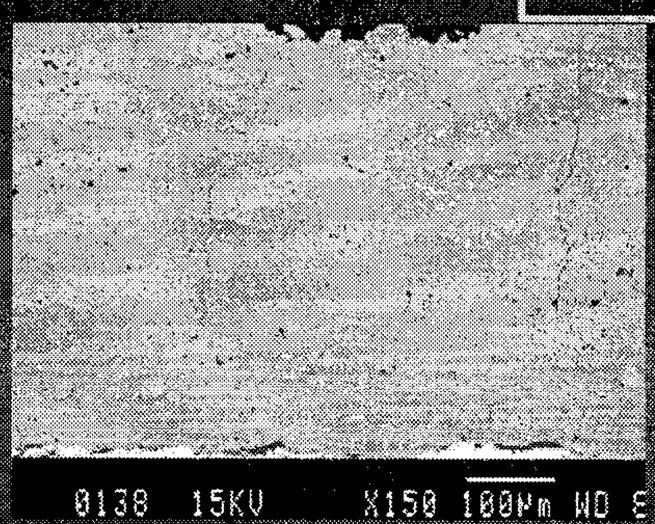
The large cracks are typically formed as stress relief due to stresses from CTE mismatch with the substrate and / or residual stresses within the coating.

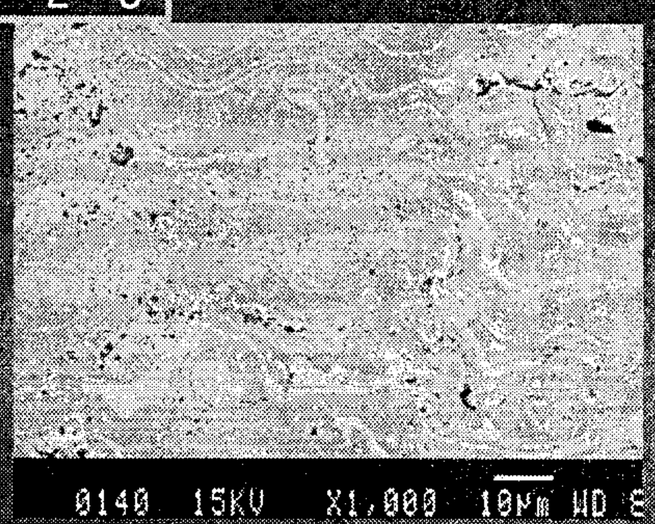
$n\text{-}TiO_2$





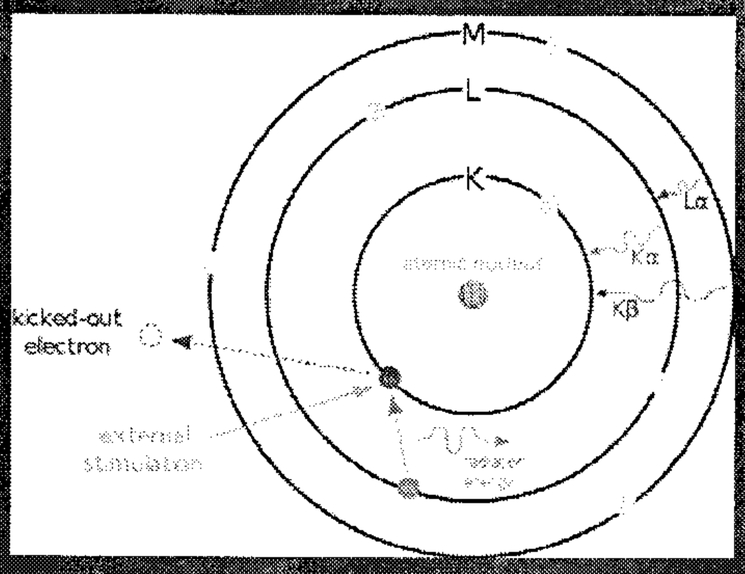
$n\text{-}TiO_2\text{-}Cr_2O_3$

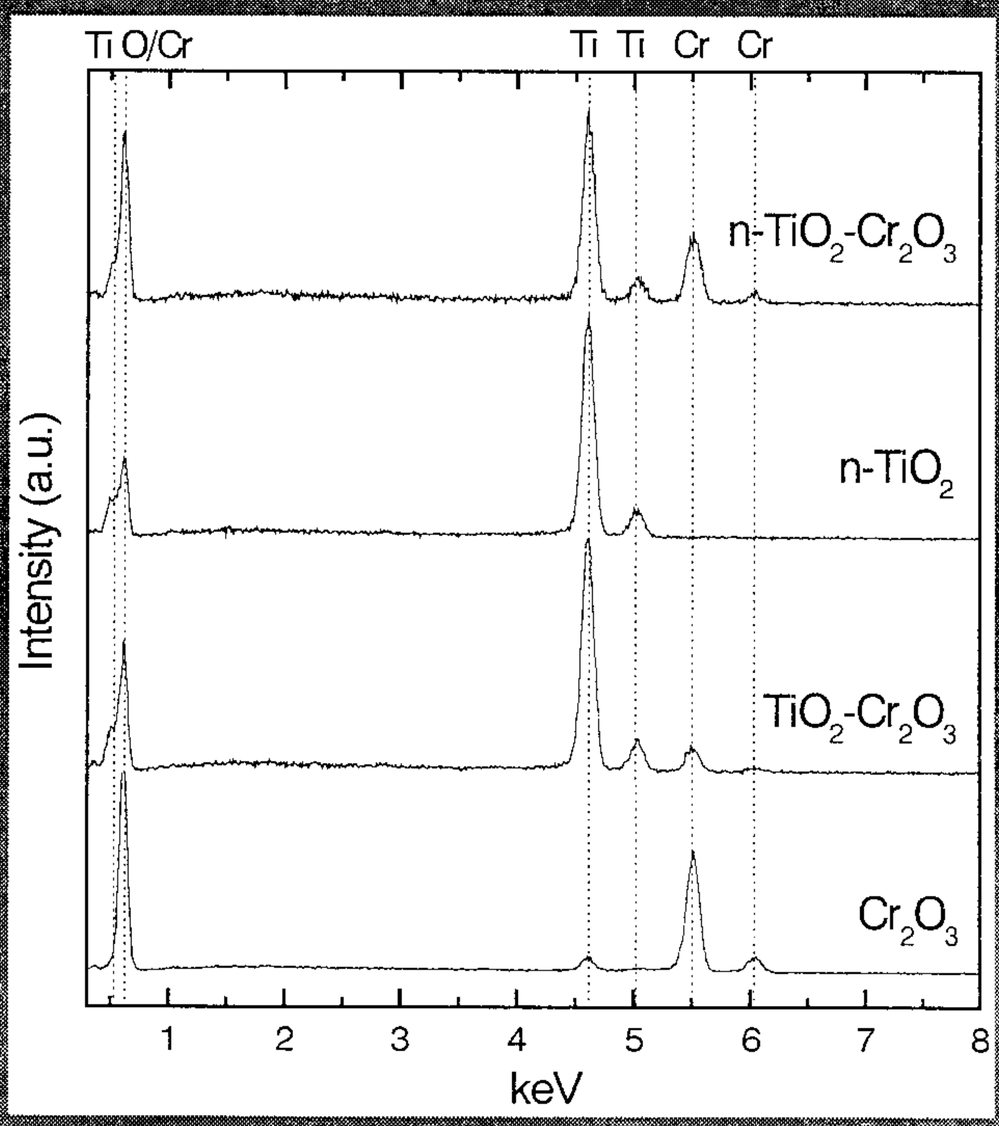




CHEMICAL CHARACTERIZATION

- Energy-dispersive X-ray spectroscopy





Peaks on X-ray spectra confirm chemical composition

MECHANICAL PROPERTIES

1) MICROHARDNESS

Microhardness measurements :

- Polished cross-sections
- Vickers Tip
- 300 gf load
- 12 indentations (straight line pattern, at the center of the coating cross section),
- Highest and lowest values removed

2) BOND STRENGTH

Shear tests (ASTM F1044).

- Instron 5582 universal testing machine

Coating	Microhardness (HV-300gf, n=10)	Shear Strength (MPa, n=5)
Cr_2O_3	1423 ± 62	> 42 ± 7 [d]
TiO_2-Cr_2O_3	912 ± 42	> 46 ± 2 [b]
n-TiO_2	729 ± 45	36 ± 2 [a]
n-TiO_2-Cr_2O_3	1200 ± 49	38 ± 5 [a]

a Adhesive failure (occurs at bond line with substrate)
b Epoxy failure (glue)
c Cohesive failure (failure within the coating)
d Mix mode of all or partial of the above.

Pure Cr_2O_3 provides the highest microhardness

Pure n-TiO_2 provides the lowest microhardness

Chromia / Titania blends are in between

Velan coatings provide the highest shear strengh (to prevent delamination during motion)

TRIBOLOGICAL PERFORMANCE

1) SLIDING WEAR RESISTANCE

25 N normal load

4.75 mm dia WC ball

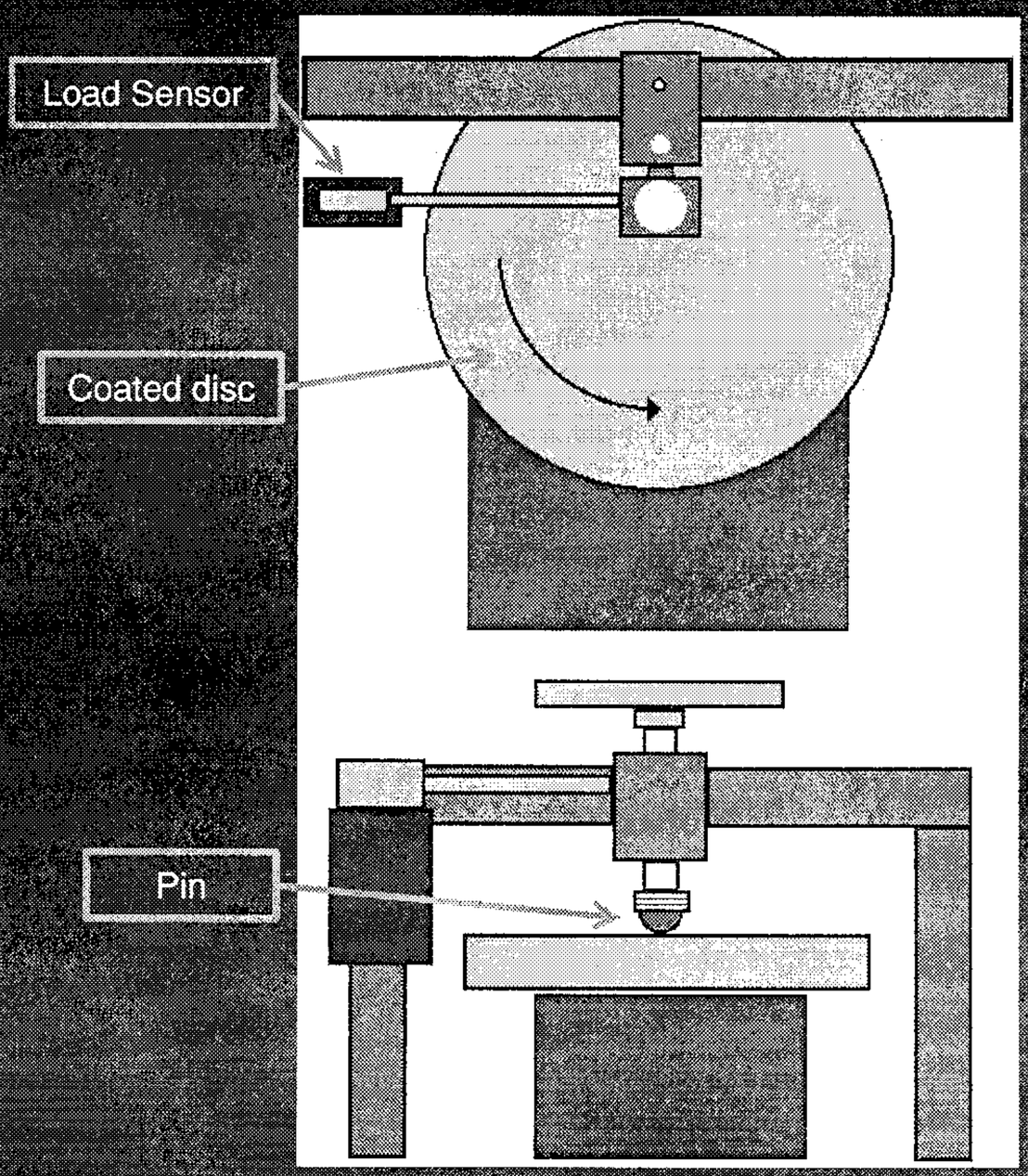
7 mm diameter wear track ring,

546 rpm rotation speed

20 cm/s Linear speed

500 m sliding distance

The coefficient of friction (COF) was recorded every second during the test.



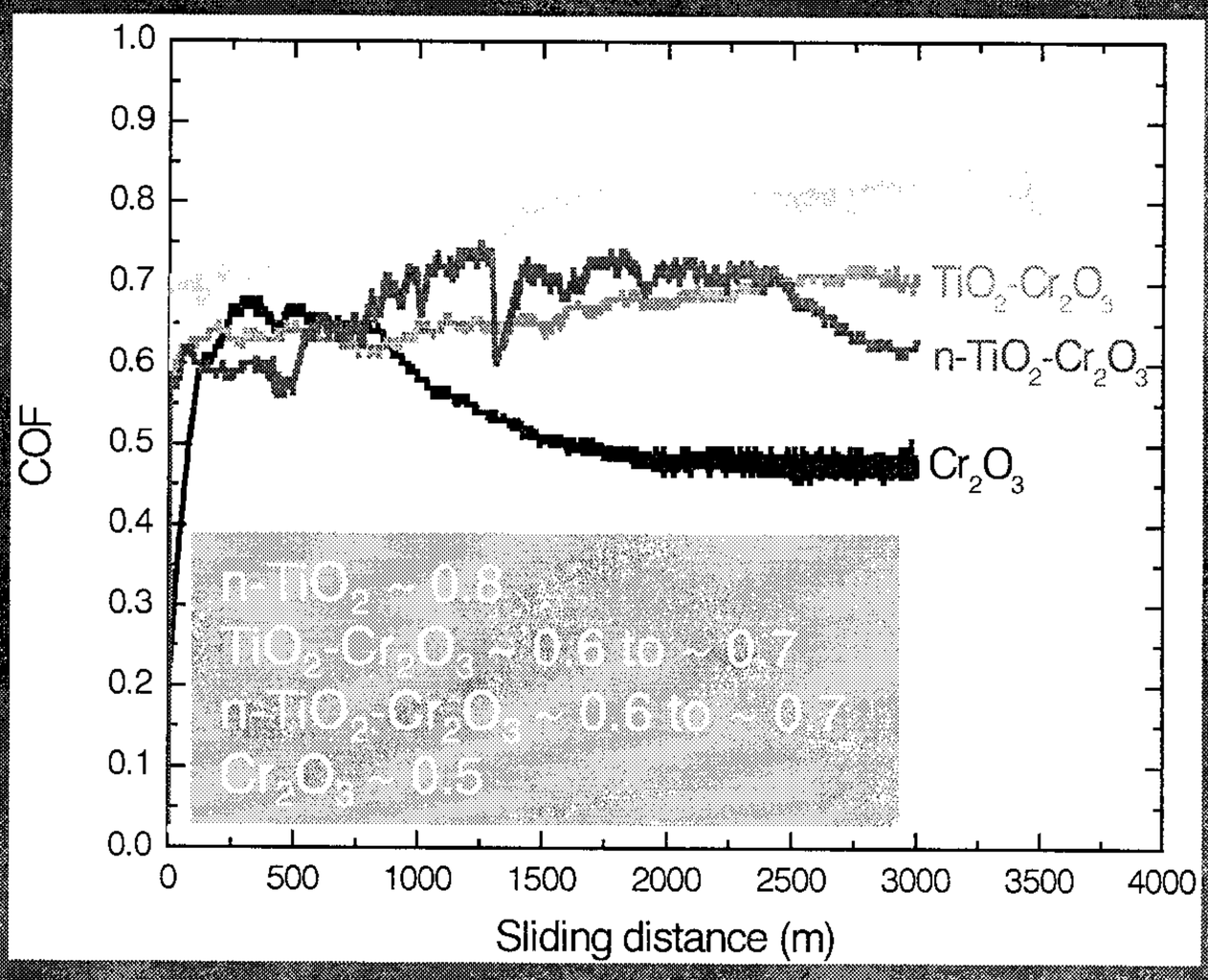
TRIBOLOGICAL PERFORMANCE

1) SLIDING WEAR RESISTANCE

25 N normal load
4.75 mm dia WC ball
7 mm diameter wear track ring,
546 rpm rotation speed
20 cm/s Linear speed
3000 m sliding distance

The coefficient of friction (COF) was recorded every second during the test.

COF correlated with microhardness measurements



TRIBOLOGICAL PERFORMANCE

1) SLIDING WEAR RESISTANCE

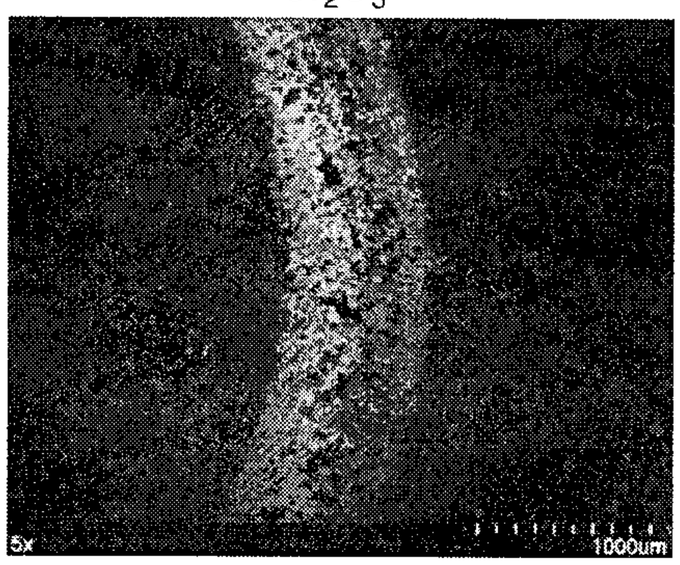
Microscopic observation of the wear tracks

n-TiO_2 has the widest and deepest wear track,

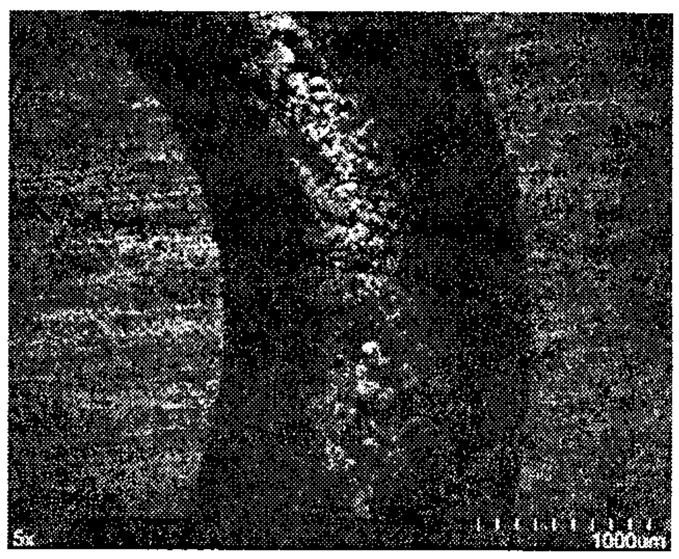
TiO_2-Cr_2O_3 has a relatively large wear track,

On the contrary, Cr_2O_3 and n-TiO_2-Cr_2O_3 show small wear scars, reflecting a mild abrasive wear process for these two coatings.

Cr_2O_3



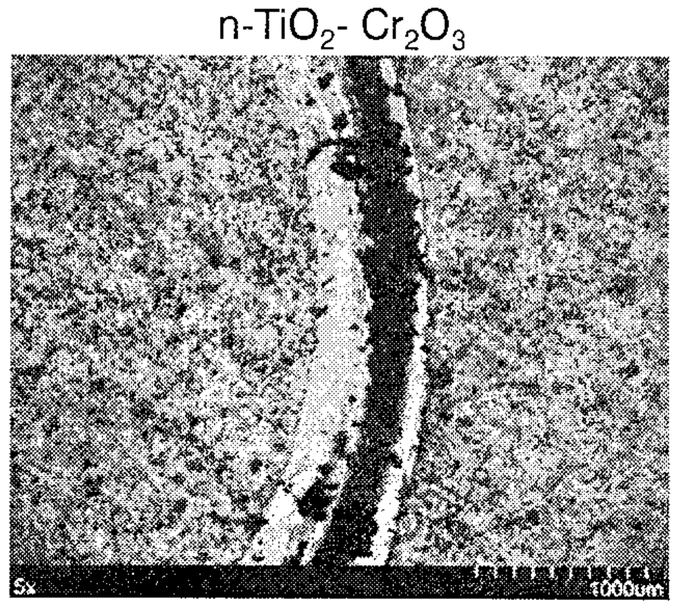
TiO_2 - Cr_2O_3



n-TiO_2



n-TiO_2- Cr_2O_3



TRIBOLOGICAL PERFORMANCE

1) SLIDING WEAR RESISTANCE

Wear rate = V/(F×s),

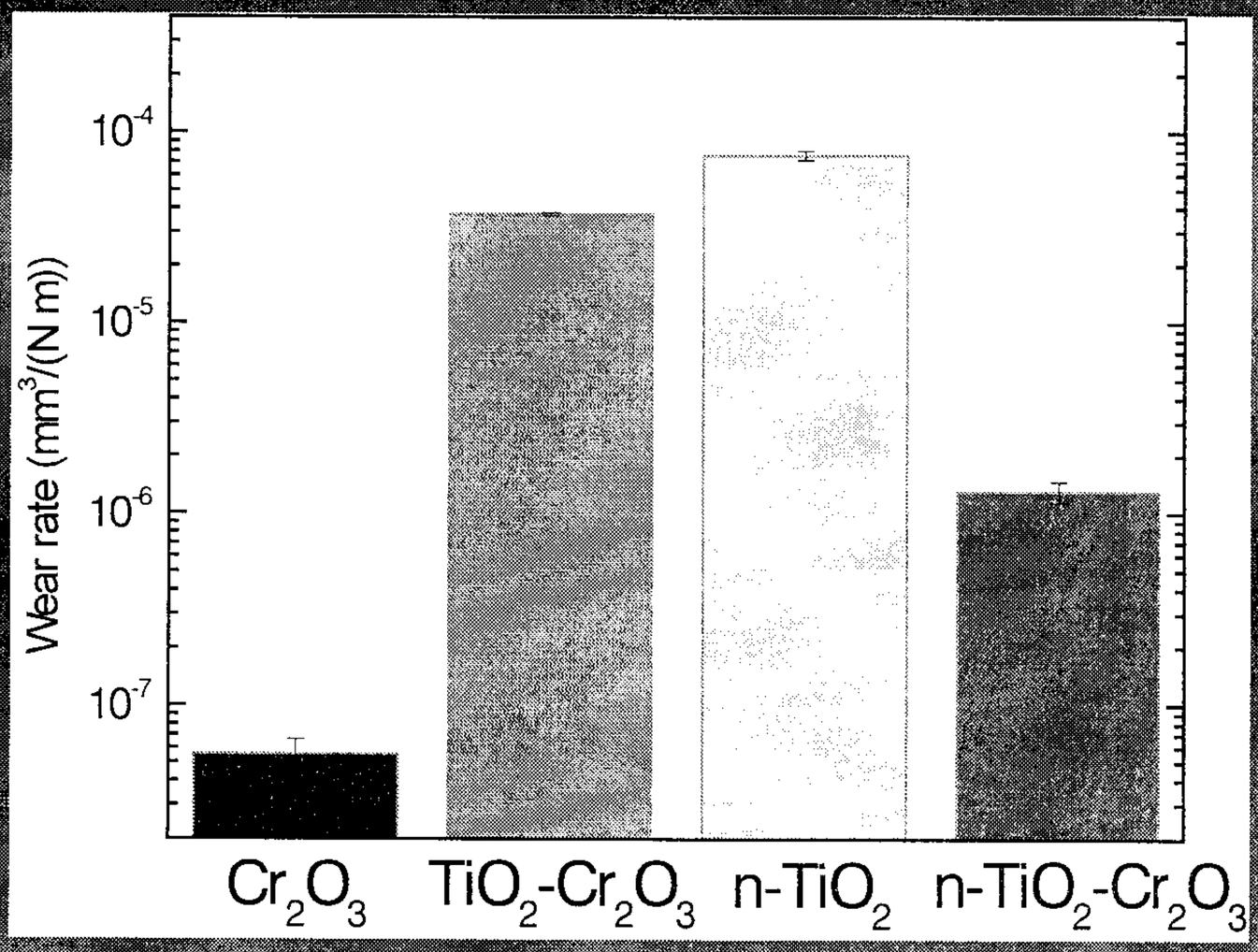
V = Worn volume

F = Normal load

S = Sliding distance

$n\text{-}TiO_2$ wear rate is 3 orders of magnitude higher compared to the Cr_2O_3 coating

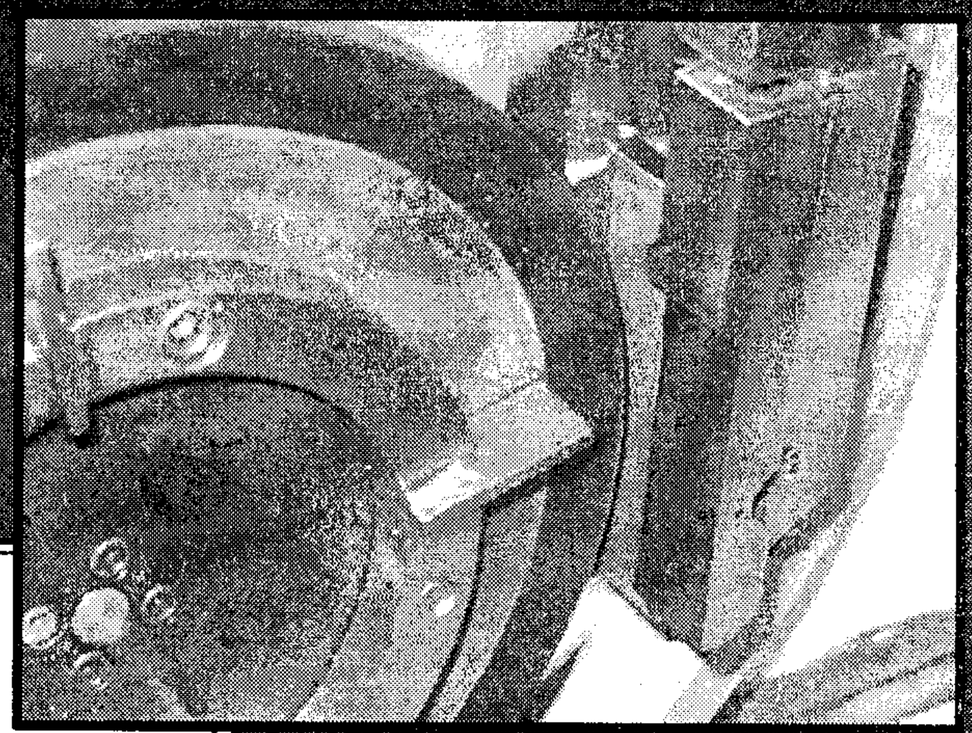
Chromia / Titania blends are in between

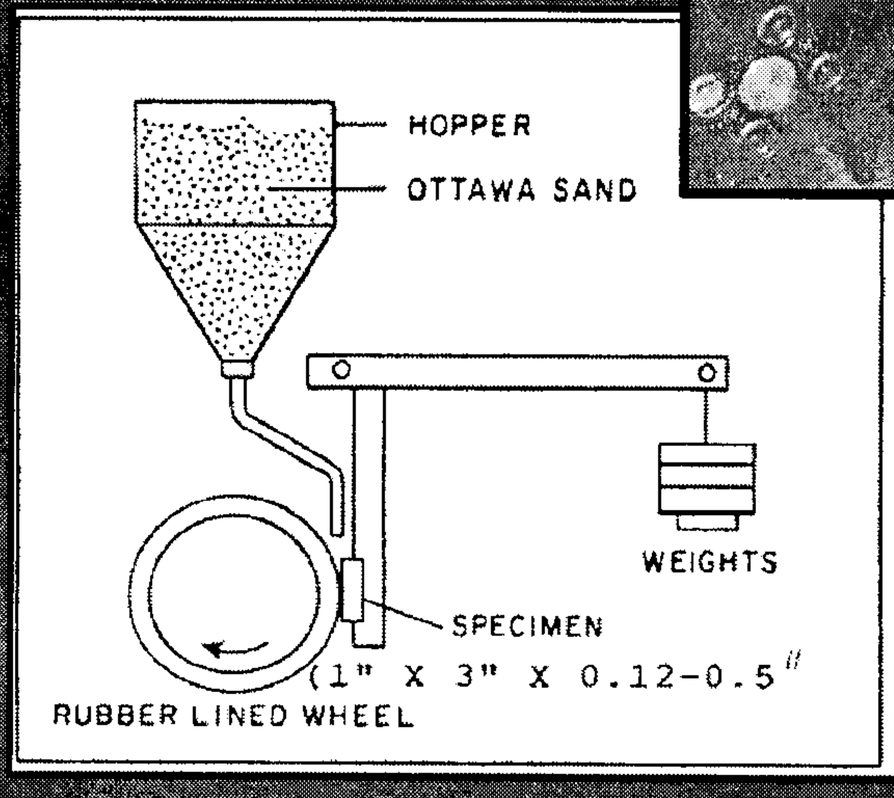


TRIBOLOGICAL PERFORMANCE

2) DRY SAND ABRASION

ASTM G65
45 N
2000 wheel revolutions
Durometer A-60 wheel
2 tests for each coating
Volume loss (profilometer)





TRIBOLOGICAL PERFORMANCE

2) DRY SAND ABRASION

ASTM G65

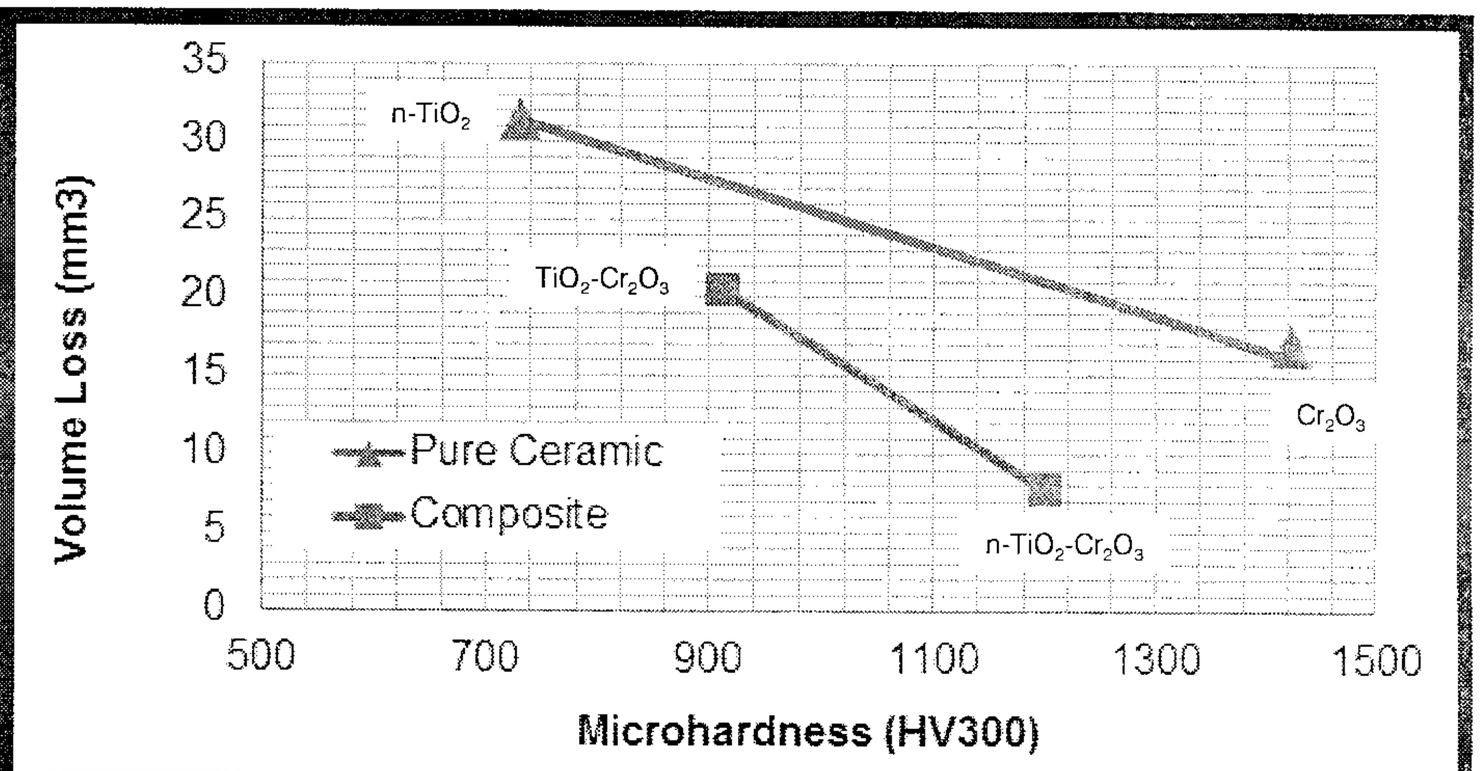
45 N

2000 wheel revolutions

Durometer A-60 wheel

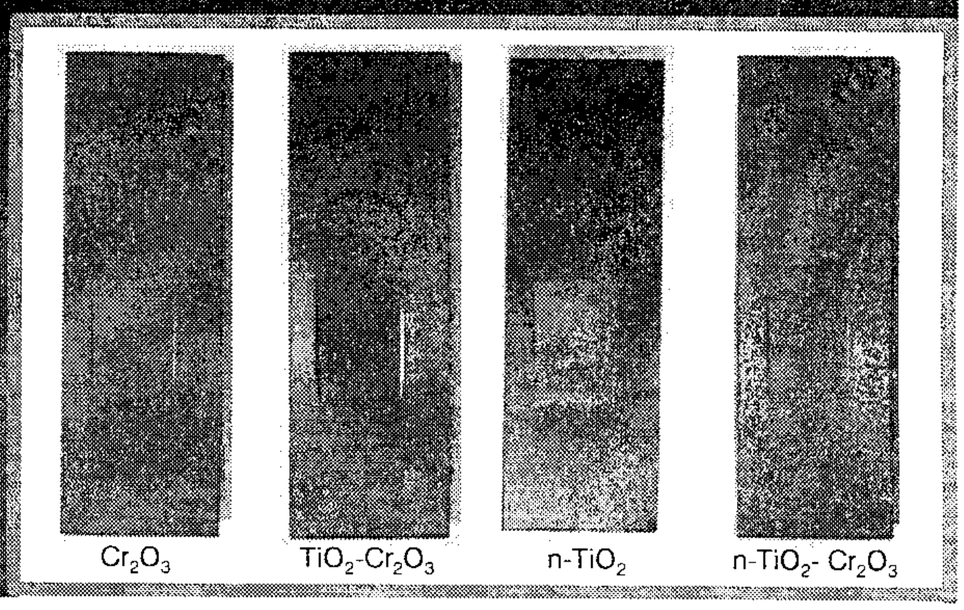
2 test for each coating

Volume loss (profilometer)



Dry sand abrasion resistance is not directly correlated to microhardness

According to our measurements, composite materials are more resistant to dry sand abrasion than pure ceramics for a given microhardness.



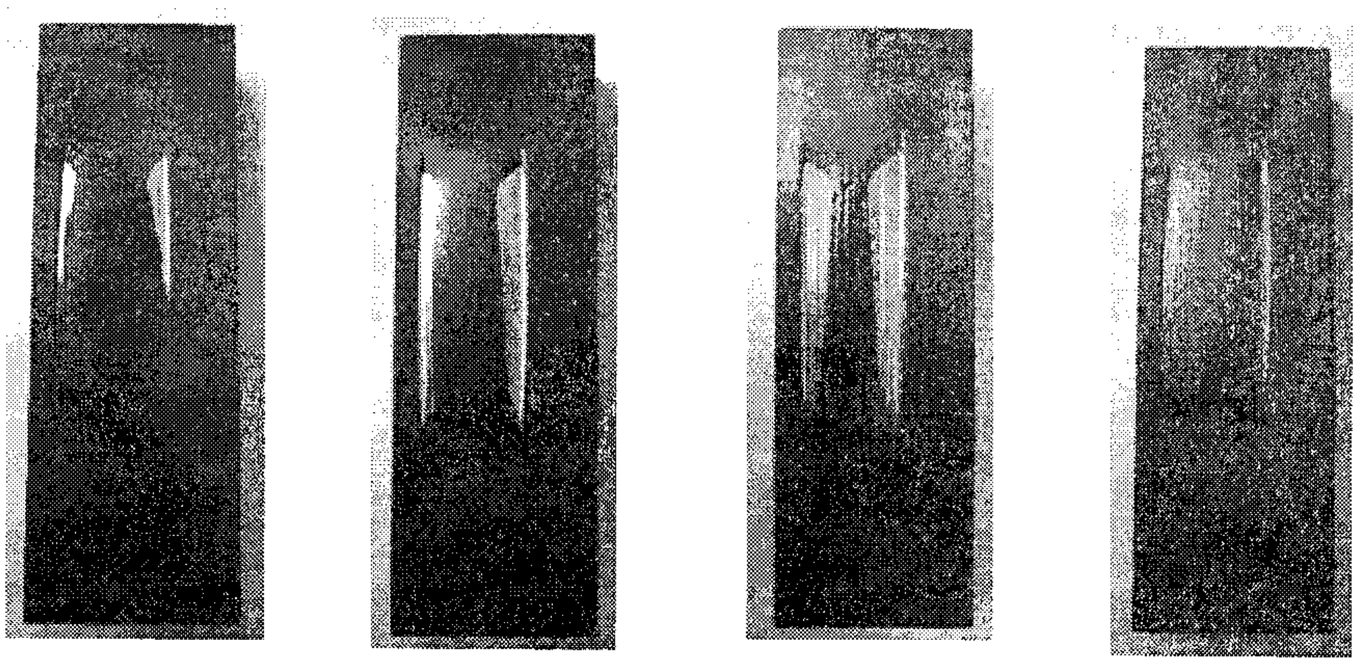
TRIBOLOGICAL PERFORMANCE

3) WET SAND ABRASION

ASTM G105-02
22 N normal load
5,000 wheel revolutions
Durometer A-60 wheel

Slurry mixture composed of rounded quartz grain sand AFS 50/70 and deionized water with respect to the ratio of 0.940 kg water / 1.500 kg sand

Mass Loss measurements



Cr_2O_3 TiO_2-Cr_2O_3 n-TiO_2 n-TiO_2- Cr_2O_3

n-TiO_2-Cr_2O_3 resisted penetration
Cr_2O_3 shows a slight penetration
TiO_2-Cr_2O_3 shows large penetration
n-TiO_2 displays the poorest performance

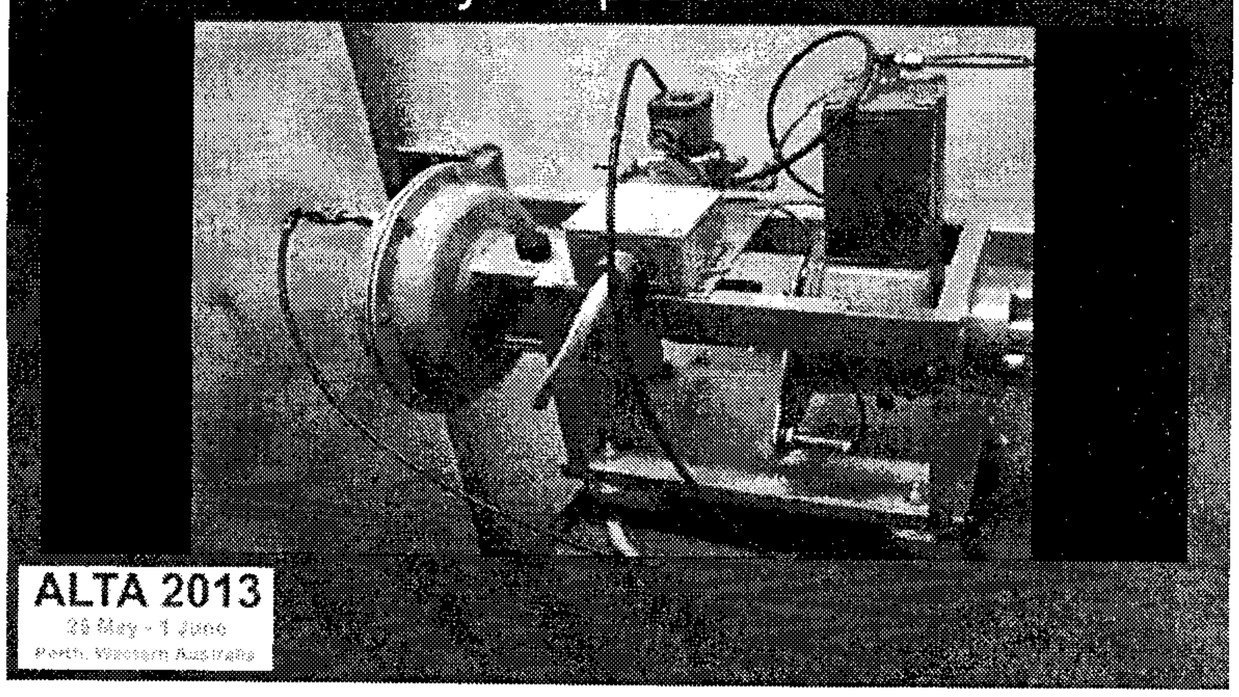
Wet sand abrasion resistance is not directly correlated to microhardness

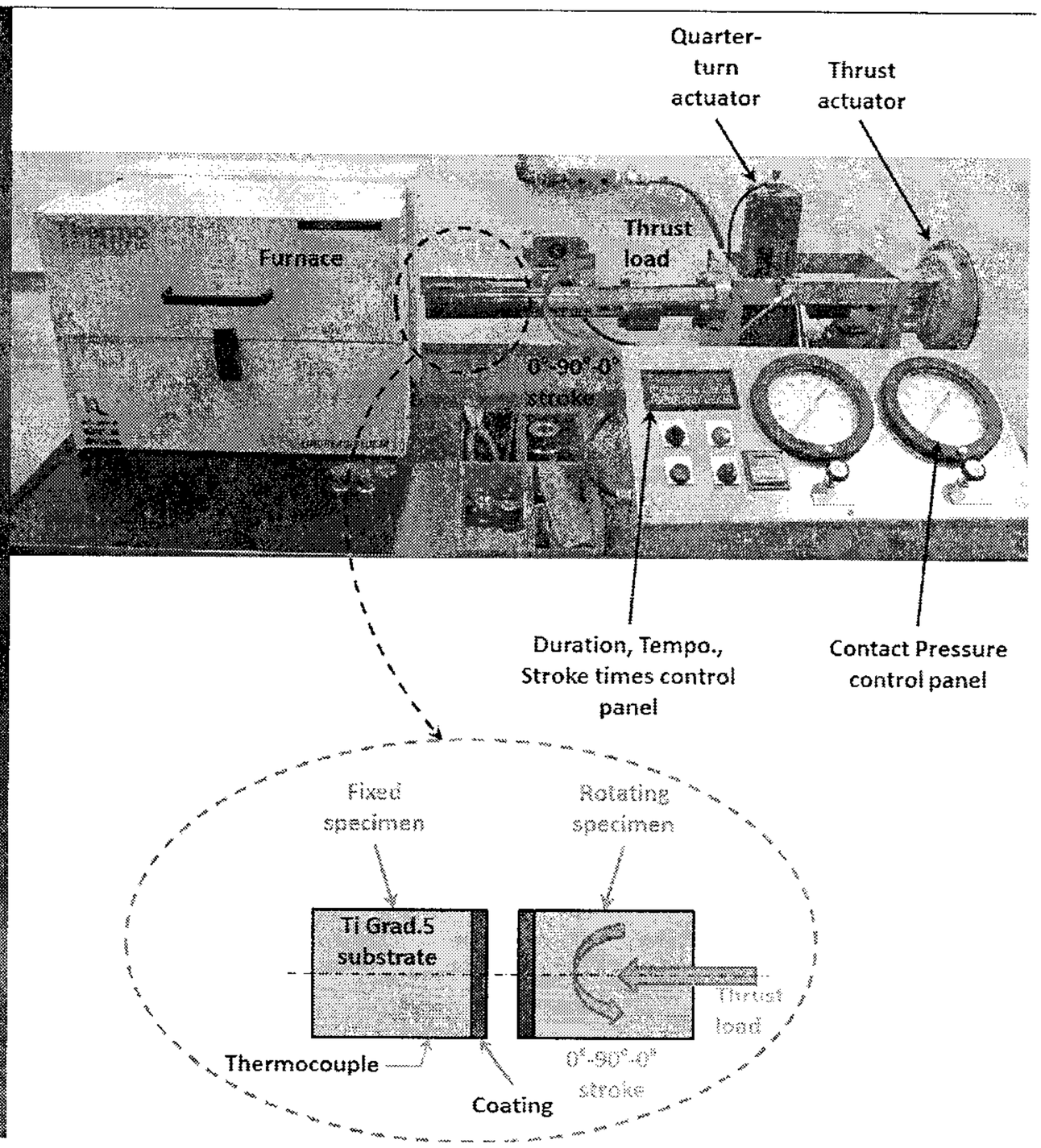
Composite materials are more resistant to Wet sand abrasion than pure ceramics for a given microhardness

TRIBOLOGICAL PERFORMANCE

4) VARIABLE TEMP. GALLING RESISTANCE

- 2 x annular samples (Ø 1.25" x 1.5")
- ¼ turn motion
- Controlled contact pressure
- Controlled temperature
- Controlled cycle speed





TRIBOLOGICAL PERFORMANCE

4) VARIABLE TEMPERATURE GALLING RESISTANCE

- Step-by-Step procedure
- After each step:
  - Visual inspection
  - mass loss measurements
- Go-to-next-step when no significant wear patterns observation

Step	Duration (nb. cycles)	Specimen temperature (°F)	Nominal contact pressure (psi)	Nb. cycles per minute	0° → 90° and 90° → 0° stroke times (s.)	Temporization at 0° and 90° position (s.)
1	50	R.T.	1,000	0.2	10	140
2	50	428	1,000	0.2	10	140
3	50	428	1,500	0.2	10	140
4	50	428	2,000	0.2	10	140

TRIBOLOGICAL PERFORMANCE

4) VARIABLE TEMP. GALLING RESISTANCE

2 x self-mated annular samples (Ø 1.25" x1.5")

¼ turn motion

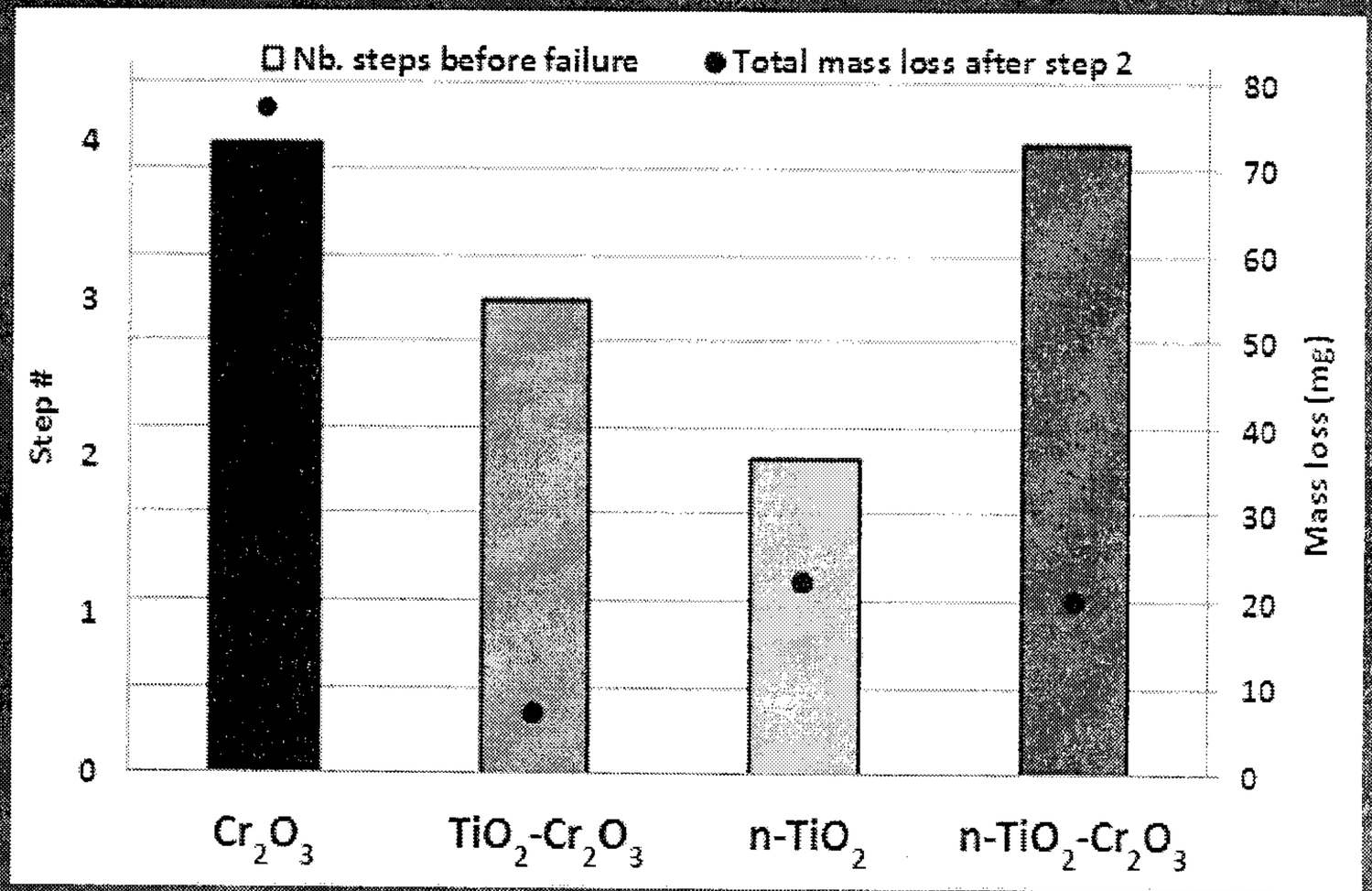
Controlled contact pressure

Controlled temperature

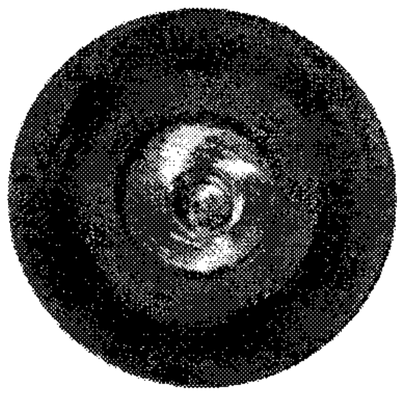
Controlled cycle speed

Visual Inspection

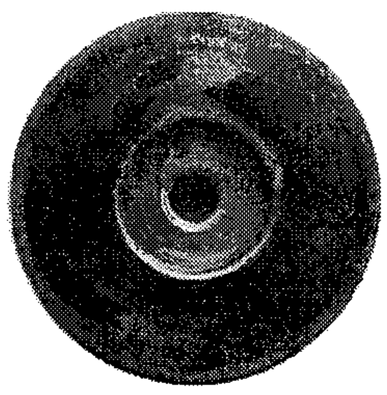
Mass Loss Measurements



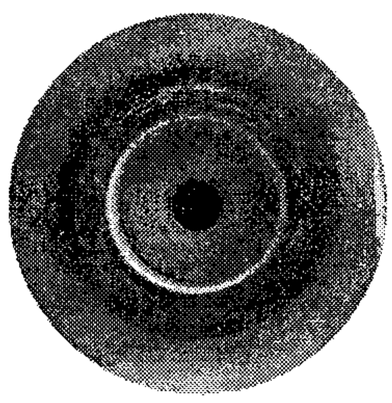
4) VARIABLE TEMPERATURE GALLING RESISTANCE



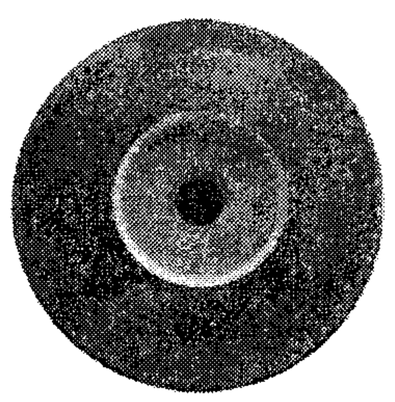
Cr_2O_3 fixed after step 4



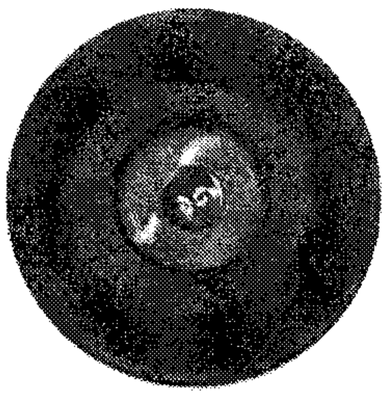
TiO_2-Cr_2O_3 fixed after step 3



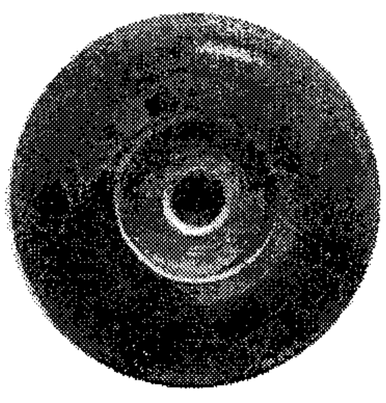
n-TiO_2 fixed after step 2



n-TiO_2-Cr_2O_3 fixed after step 4



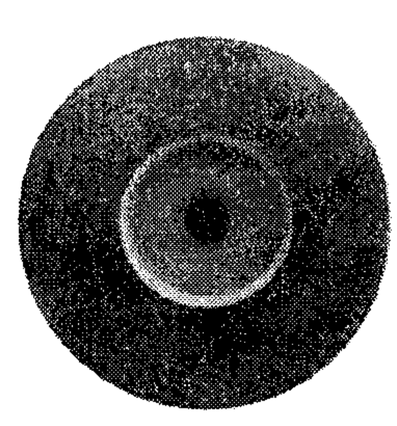
Cr_2O_3 rotating after step 4



TiO_2-Cr_2O_3 rotating after step 3



n-TiO_2 rotating after step 2

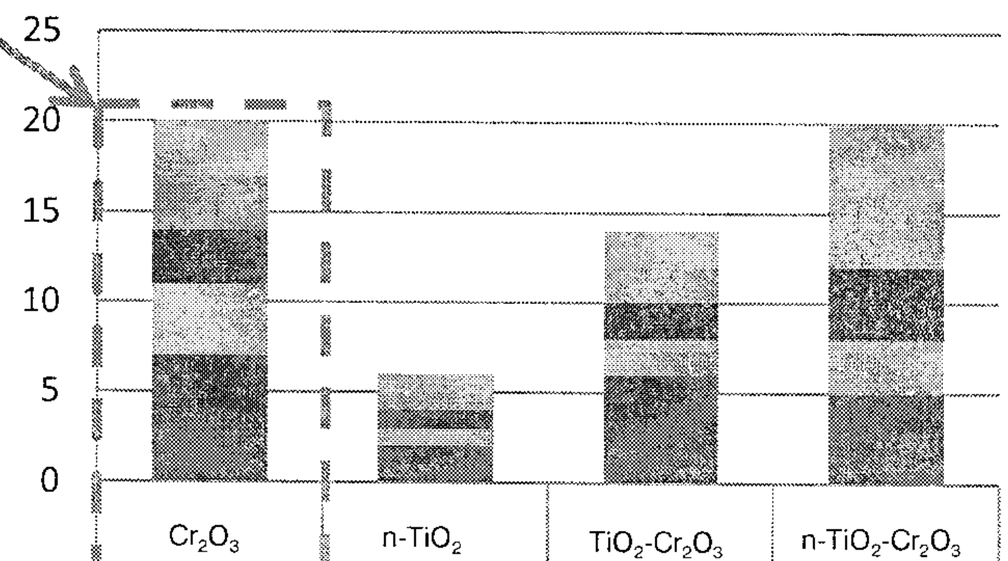


n-TiO_2-Cr_2O_3 rotating after step 4

CONCLUSION

For benchmak only
Not recommended for HPal

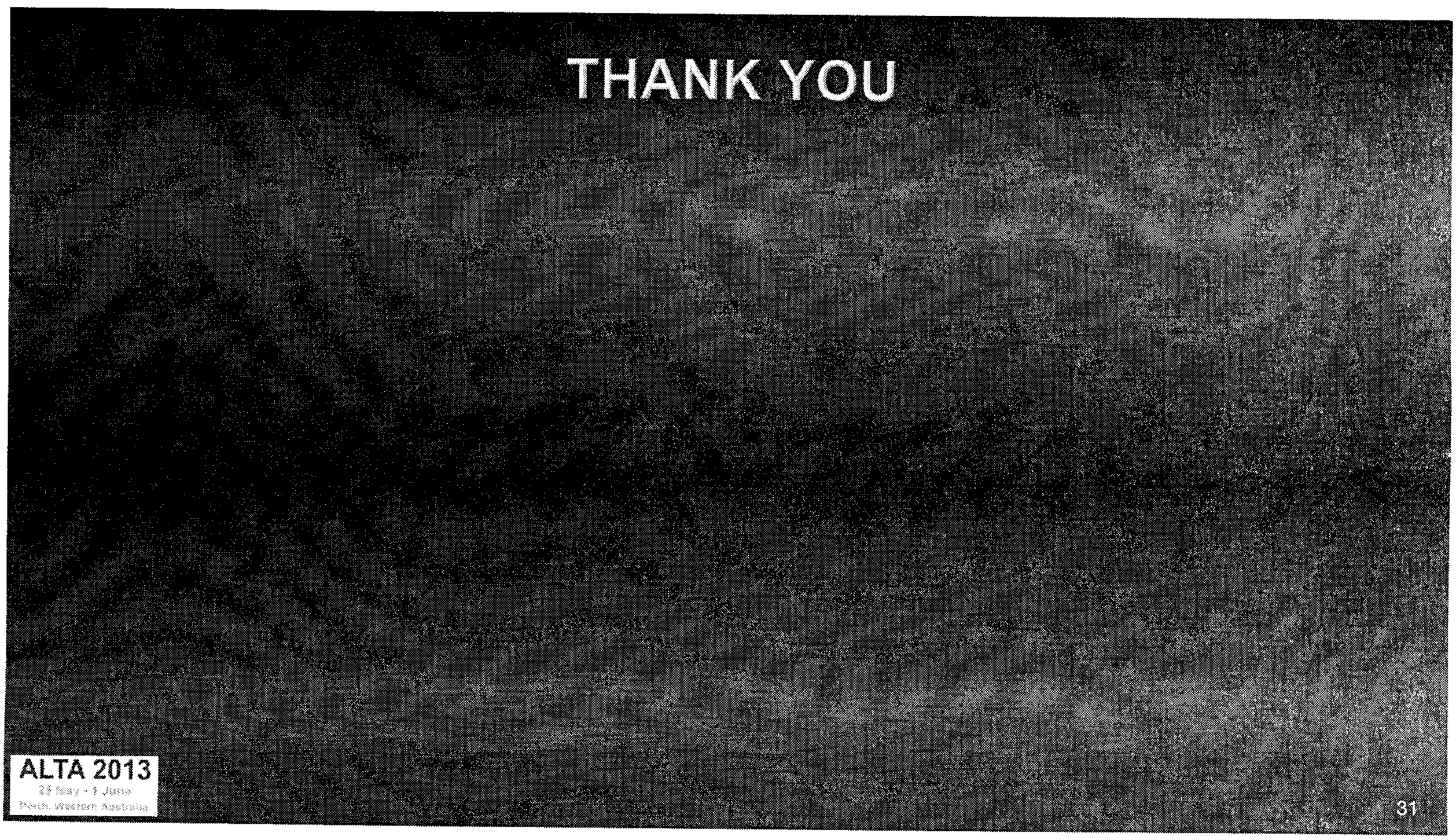
Tribological & Mechanical Performance Ranking
4 = Best
1 = Worst



	Cr_2O_3	n-TiO_2	TiO_2-Cr_2O_3	n-TiO_2-Cr_2O_3
Variable Temp. Galling	3	1	2	4
Wet Sand Abrasion	3	1	2	4
Dry Sand Abrasion	3	1	2	4
Sliding Wear Resistance	4	1	2	3
Bond Strength	3	1	4	2
Microhardness	4	1	2	3

CONCLUSION

- Pure Cr_2O_3 blend has shown the highest hardness, best sliding wear resistance and COF but a relatively poor abrasive performance,
- Cr_2O_3-TiO_2 and n-TiO_2-Cr_2O_3 blends have offered superior resistance during both dry and wet abrasions tests,
  - n-TiO_2 has offered deceptive performance,
  - The synergy between Cr_2O_3 and TiO_2 yields to abrasion performance exceeding the one of each individual.


THANK YOU
ALTA 2013
28 May - 1 June
Perth, Western Australia